

02

154613

RI 9457

REPORT OF INVESTIGATIONS/1993

PLEASE DO NOT REMOVE FROM LIBRARY

LIBRARY
SPOKANE RESEARCH CENTER
RECEIVED

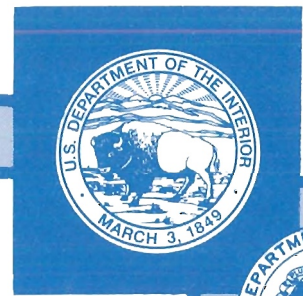
MAY 11 1993

US BUREAU OF MINES
E. 315 MONTGOMERY AVE.
SPOKANE, WA 99207

Predicting Flow Characteristics of a Lixiviant in a Fractured Crystalline Rock Mass

By Nadia C. Miller

UNITED STATES DEPARTMENT OF THE INTERIOR



BUREAU OF MINES

Mission: As the Nation's principal conservation agency, the Department of the Interior has responsibility for most of our nationally-owned public lands and natural and cultural resources. This includes fostering wise use of our land and water resources, protecting our fish and wildlife, preserving the environmental and cultural values of our national parks and historical places, and providing for the enjoyment of life through outdoor recreation. The Department assesses our energy and mineral resources and works to assure that their development is in the best interests of all our people. The Department also promotes the goals of the Take Pride in America campaign by encouraging stewardship and citizen responsibility for the public lands and promoting citizen participation in their care. The Department also has a major responsibility for American Indian reservation communities and for people who live in Island Territories under U.S. Administration.

Report of Investigations 9457

Predicting Flow Characteristics of a Lixiviant in a Fractured Crystalline Rock Mass

By Nadia C. Miller

**UNITED STATES DEPARTMENT OF THE INTERIOR
Bruce Babbitt, Secretary**

BUREAU OF MINES

Library of Congress Cataloging in Publication Data:

Miller, Nadia C.

Predicting flow characteristics of a lixiviant in a fractured crystalline rock mass /
by Nadia C. Miller.

p. cm. — (Report of investigations / Bureau of Mines, United States Department
of the Interior; 199); 9457.

Includes bibliographical references (p. 23).

1. Leaching—Mathematical models. 2. Rocks—Permeability—Mathematical models. 3. In situ processing (Mining)—Mathematical models. I. Title. II. Series: Report of investigations (United States. Bureau of Mines); 199. 9457.

TN23.U43 [TN278.3] 622 s—dc20 [622'.22] 92-21551 CIP

CONTENTS

Page

Abstract	1
Introduction	2
Description of problem	2
Purpose and objectives	3
Research site description	3
Research procedure	3
Acknowledgments	4
Fluid flow through fractured media	4
Theory	4
Methods of measuring flow characteristics of fractured media	7
Methods of analysis	8
Geology of Edgar Mine site	8
Historical geology	8
Site geology	9
Local hydrology	9
Hydrogeology of Edgar Mine	9
Research design and implementation	10
Methods	10
Geologic mapping	10
Well field design	10
Drilling and core recovery	10
Core logging	11
Overall geologic interpretation and analysis	12
Hydrologic testing	15
Fracture flow model and data analysis	19
Conclusions and recommendations	22
References	23

ILLUSTRATIONS

1. General location of Colorado School of Mines Experimental Mine	2
2. Plan view of Edgar Mine	3
3. Plan view of experimental stope site with locations of test wells	4
4. Continuum and noncontinuum models	5
5. Pore canal system	5
6. Parallel plates illustrating Cubic law	7
7. Geology of experimental stope site	9
8. Core orientor	11
9. Goniometer	11
10. Rose diagram of core fracture dip orientations	12
11. Blast damage	12
12. Probability distribution of fracture orientations	13
13. Probability distribution of fracture spacing	13
14. Apparent spacing versus actual spacing	14
15. Probability distribution of fracture trace length	14
16. Probability distribution of fracture aperture	14
17. Probability distribution of fracture hydraulic conductivities from research by Office of Crystalline Rock Depositories	14
18. Probability distribution of fracture hydraulic conductivities from air packer tests	15
19. Schmidt net from Edgar Mine fracture data	15
20. PLUME model dispersivities versus rose diagram for stope site fracture dip orientations	16

ILLUSTRATIONS

	<i>Page</i>
21. Equipment setup for air packer tests	16
22. Equipment setup for water packer tests	16
23. Example of raw data from air packer test	16
24. Example of data to be used for curve matching	17
25. Type curves for drill stem tests or slug tests	17
26. Curve matching example	17
27. Avenues of air loss during air packer tests	18
28. Direction of ground water velocity as calculated by PLUME model	19
29. Concentration versus distance with time as third variable	20
30. Peak concentration versus dispersivity after 1 year	20
31. Peak concentration versus fracture spacing after 1 year	20
32. Peak concentration versus ground water velocity after 1 year	21
33. Peak concentration versus porosity after 1 year	21
34. Map of Idaho Springs area showing Big Five Tunnel, fault, and vein locations	22
35. Predicted flow direction of lixiviant plume	22

TABLES

1. Hydraulic conductivities from water packer tests	18
2. Hydraulic conductivities from air packer tests	18

UNIT OF MEASURE ABBREVIATIONS USED IN THIS REPORT

ft	foot	m	meter
ft/d	foot per day	min	minute
ft/yr	foot per year	ppm	part per million
g	gram	psi	pound per square inch
in	inch		

PREDICTING FLOW CHARACTERISTICS OF A LIXIVANT IN A FRACTURED CRYSTALLINE ROCK MASS

By Nadia C. Miller¹

ABSTRACT

In situ metals research to characterize the hydrology of a fractured crystalline rock mass in underground mine stopes is discussed. The objective of this study was to find the potential direction, velocity, and concentrations of a lixiviant plume, should leaching solvents (lixivants) escape from a test stope.

The study was conducted by the U.S. Bureau of Mines at the Colorado School of Mines Experimental Mine in Idaho Springs, CO. Since this was a method evaluation site, the lixiviant was simulated using water and acceptable tracers. The site is located in moderately fractured Precambrian migmatite-biotite gneisses of the Idaho Springs Formation. The data required for the characterization were obtained from geologic maps and reports, core logs, and air and water permeability tests. The acquired data were analyzed and applied to a computer model that calculated the characteristics of a lixiviant plume originating at the stope.

A sensitivity analysis showed that dispersivity, ground water velocity, fracture porosity, and fracture spacing had notable effects on the concentration of the plume. Assuming a saturated rock mass, the lixiviant plume would disperse to undetectable levels in a very short time because of a high fracture density at the mine site.

¹Geological engineer, Denver Research Center, U.S. Bureau of Mines, Denver, CO.

INTRODUCTION

DESCRIPTION OF PROBLEM

New and innovative methods to economically mine metal ore and minimize mining development time, materials handling, conventional milling, and surface waste disposal are currently being sought by the minerals industry. The U.S. Bureau of Mines is conducting research on in situ stope leaching, which could potentially meet the goals of modern mining techniques by making use of low-grade ore deposits and minimizing the transport of tons of rock. Although this method can be economical in some respects, it poses a challenge in controlling leaching solutions.

The process of ore leaching consists of fragmenting ore, introducing chemical lixivants to extract metals, and collecting and processing the metal-bearing solution. The goal of the in situ stope leaching study is to determine the feasibility of applying this method to stopes located in active underground mines. In stope leaching, existing stopes can be used by filling them with low-grade ore and leaching the stopes for metal recovery, or new stopes may

be developed by fragmenting low-grade ore in place within the area of the stope.

Critical to the success of stope leaching is solution control of the lixiviant. The Bureau selected the Edgar Mine in Idaho Springs, CO, to assess the requirements of solution control (fig. 1). Methods to characterize a rock mass for the application of in situ leaching and methods to develop stopes for leaching were evaluated at the site. Leaching chemicals were not used at the site. In their place, water and approved tracers simulated chemicals in experiments.

The site is located in moderately fractured metamorphic rock of the Idaho Springs-Central City Mining District. Because igneous and metamorphosed crystalline rock matrices have extremely low hydraulic conductivities, the fractures within the rock mass influence the movement of fluids away from the stope leaching area. Among the most critical rock characteristics related to in situ stope leaching are the hydrologic properties of the rock mass. An idea of

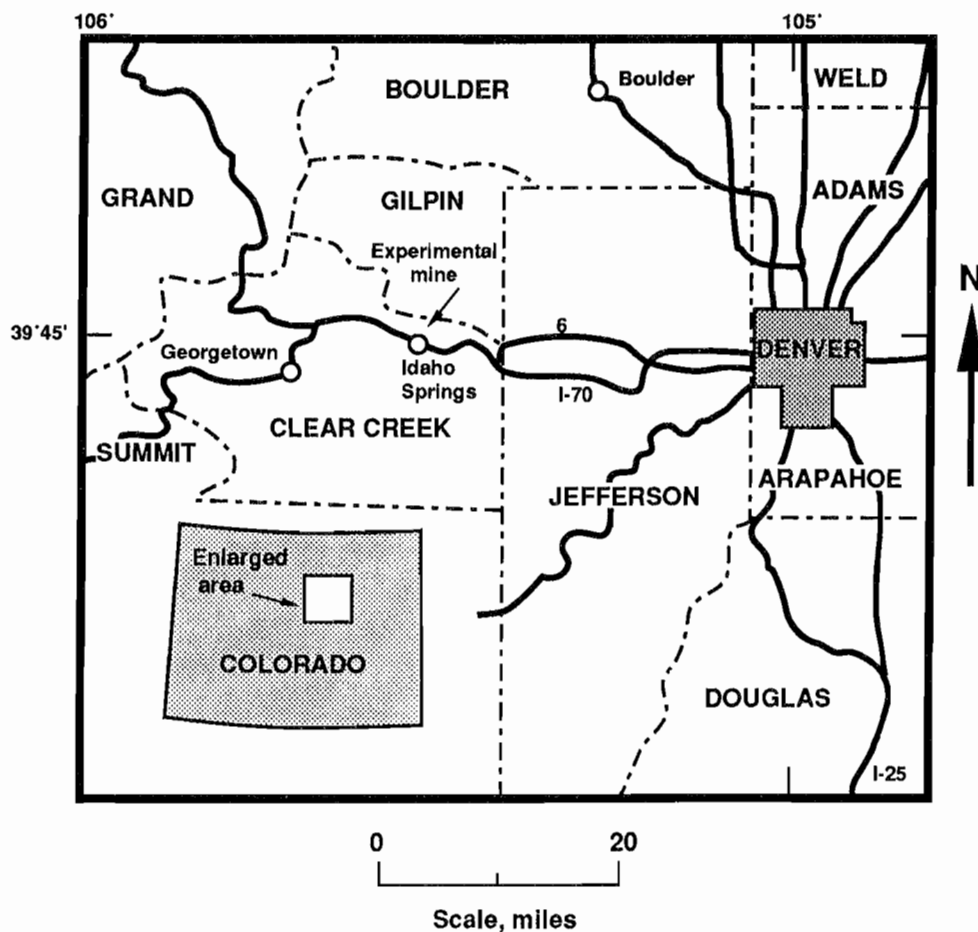


Figure 1.—General location of Colorado School of Mines Experimental Mine (Edgar Mine).

how the lixiviant plume will behave in the rock mass would be a key component in the environmental assessment of the leaching process.

PURPOSE AND OBJECTIVES

The evaluation of the in situ leaching method involves several areas of study: metallurgy, geology, hydrogeology, geochemistry, blasting, and mine design. The purpose of this study was to characterize and model the fracture hydrology adjacent to an underground mine stope to be used for leaching ore. To do this it was necessary to have a detailed understanding of the hydrogeology of the stope site regarding the dispersion of the leach solution through fracture sets within the stope environment. The fracture hydrology of the site was modeled assuming saturated conditions that would be present concurrent with the leaching process, and emphasizing the dispersion and migration time of the leach solution. To understand how the leach solution will be attenuated through the fracture network, the following objectives were met:

- Understand the theory of fluid flow through fractured geologic media;
- Compile available information on fracture characteristics in the Idaho Springs area and the Edgar Mine;
- Map the detailed geology of the stope area (map the room and drill holes) to understand the nature of the fractures;
- Interpret the structural geology of the area in general and how it applies to local hydrogeology;
- Obtain rock system permeabilities at the stope site; and
- Use a computer model to model fluid flow and dispersion.

RESEARCH SITE DESCRIPTION

The project site is located at the Colorado School of Mines Experimental Mine (the Edgar Mine) (Sec. 26 and 35, T. 35 N., R. 73 W.), located approximately one-fourth mile north of Idaho Springs, CO. The experimental stope (elevation of approximately 7,950 ft) is approximately 1,000 ft northwest of the Miami Tunnel portal (fig. 2). The stope site and access were excavated during the spring and winter of 1989. The stope is 6 ft in diameter and 27 ft in height. To obtain fracture characteristics information and permeability and dispersion data for future studies, a set of four vertical observation wells, wells 1, 2, 3, and 4, and one inclined well, well 5, were drilled in and around the future stope, extending to depths of 20 and 40 ft (fig. 3). A set of three 40-ft monitoring wells, wells 6, 7, and 8, were drilled below the stope site (fig. 3). Wells 1, 2, 3, 4, 5, and 7 were used to obtain fracture information.

The Edgar Mine is an ideal environment for testing and improving new mining technology. Because it has been a research and educational facility for more than 50 years, there is a wealth of information on the geologic characterization of the mine. In addition, the mine is not producing ore; therefore, the environment in which tests are conducted is relatively controlled. Although the leaching phase of this project cannot be conducted at the Edgar Mine, methods and procedures can be evaluated.

RESEARCH PROCEDURE

Solution control of the lixiviant is a major concern in any leaching operation. The lixiviant, if it were to flow out of the target ore zone, would most likely travel through fractures surrounding the stope. By predicting the flow of the lixiviant through the use of an analytic computer model, PLUME² (23),³ a general estimation was

²Reference to specific products does not imply endorsement by the U.S. Bureau of Mines.

³Italic numbers in parentheses refer to items in the list of references at the end of this report.

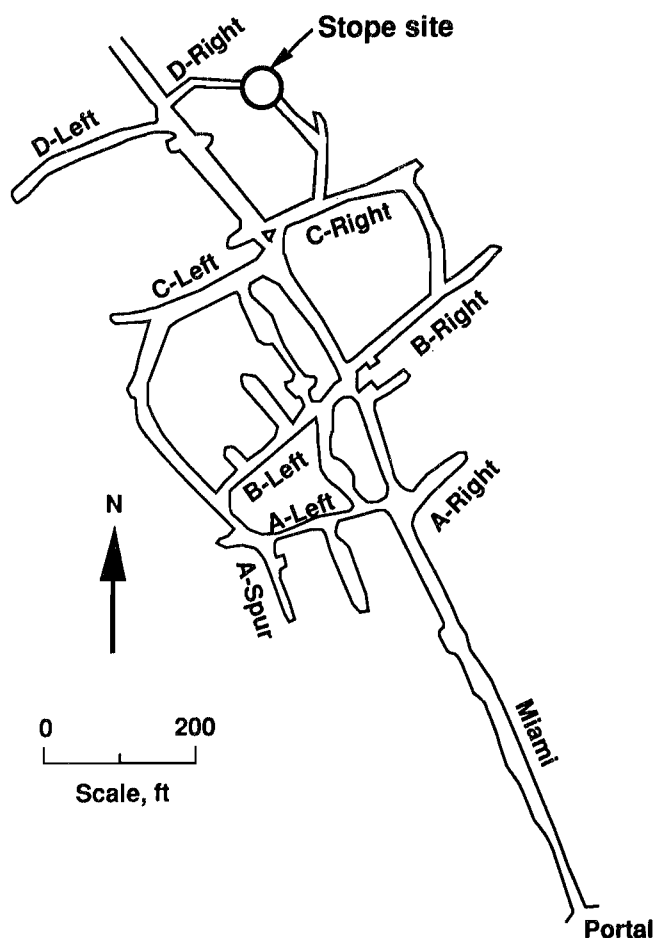


Figure 2.—Plan view of Edgar Mine.

made as to where the lixiviant is most likely to flow. In addition, estimations of how long it will take for the lixiviant to reach water resources in the area and the concentration of the lixiviant along a particular flow path were made.

In order to predict the fate of the lixiviant, the following steps were taken:

- Literature was reviewed concerning structural geology and hydrogeology in the Idaho Springs area;
- Literature concerning the theory of fracture flow was also reviewed;
- Fracture characteristics, such as orientation, spacing, and aperture, as well as geology were mapped in all drifts adjacent to the stope room (the stope room itself was mapped in much more detail);
- Equipment was selected for hydrologic testing;
- A well field was designed for the purpose of obtaining core for mapping and for later hydrologic testing;
- Hydrologic tests were conducted to find rock system hydraulic conductivities, dispersion coefficients, and the potential hydraulic gradient;
- Fracture characteristics were analyzed, using probability theory and statistics, to determine randomness and distributions, and to select parameters as input into the model;
- Fracture characteristics and regional structural geology were interpreted for use in the model; and
- The model was run and sensitivity analyses were performed on the results.

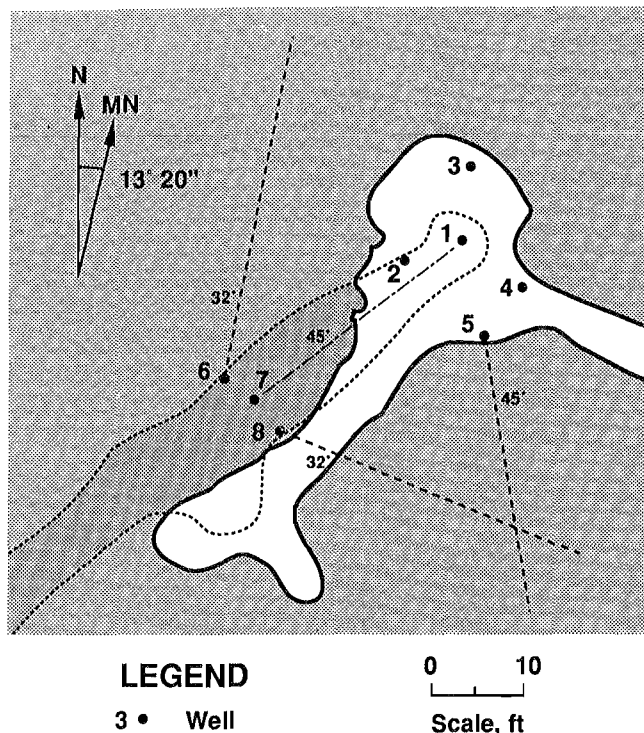


Figure 3.—Plan view of experimental stope site with locations of test wells.

ACKNOWLEDGMENTS

The author wishes to thank Dr. James Kunkel, adjunct professor at the Colorado School of Mines Geology

Department, for the guidance provided over the course of this study.

FLUID FLOW THROUGH FRACTURED MEDIA

Although fluid flow in granulated materials is fairly well understood, analysis of fluid flow through fractured media can present some problems in flow interpretation. Opinions differ as to whether flow through each fracture should be analyzed or if the fractures can be assumed to behave as pores in a granular medium. In either case, flow is assumed to be laminar and nonturbulent, since Darcy's law is applied (11, 43).

THEORY

There are two basic approaches to interpret dispersion of the lixiviant away from the leach stope. One approach, the noncontinuum model (fig. 4), analyzes each fracture in the network, one at a time. This approach is also known as the discrete fracture model and is based on the principles of fluid mechanics, which describe laminar flow in

a fracture of known geometry (21, 25, 38). The other approach, the continuum model (fig. 4), assumes a fracture network can be replaced by a representative continuum in which spatially defined hydraulic values can be assigned; thus the network behaves as if it were a porous medium (12, 16, 20, 36, 39, 41).

Several problems are associated with the many variations of the discrete fracture model. Although this method would seem to be the most accurate, it is very difficult to model, because it is difficult to assess spatial and temporal changes in fracture properties. In nature, fracture apertures vary with location along the length of the fracture, and one single fracture may have a high degree of tortuosity. Some fractures also intersect and some may not be continuous. In addition, it is assumed that the aperture of the fracture is narrow enough to allow laminar flow, in order that Darcy's law may be applied (11). This

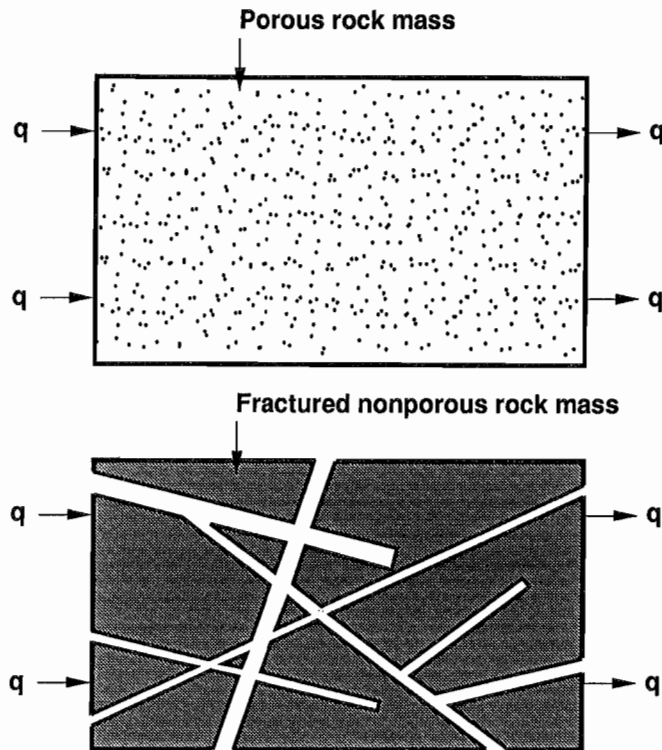


Figure 4.—Continuum (top) and noncontinuum (bottom) models, where 'q' is flow.

approach can be used advantageously in a rock mass with a very low fracture density, where individual fractures can be analyzed.

Although continuum models assume that fractured rock behaves as an equivalent porous media, some continuum models emphasize that the flow is actually controlled by fractures. Because dispersion of fluids through a fractured rock mass is generally controlled by the geometry of the fracture network and the hydraulic gradient, it would be ideal to model this situation in more than one dimension and to have variable aperture openings and lengths. Several continuum models attempt to do this by making various assumptions concerning the governing properties of flow (29). In order to evaluate the behavior of the lixiviant in the rock adjacent to the experimental stope, a continuum model, the "de Josselin de Jong" model, was used. De Josselin de Jong and Way (13) developed equations that use probability theory (9) to relate the dispersion of particles to fracture characteristics, hydraulic gradient, and directional hydraulic conductivity. The de Josselin de Jong model is based on these properties. This model assumes a pore canal system for the fracture network in which a certain particle will choose a certain path, taking into account the anisotropic nature of the media (fig. 5). Many particles dispersing from a source will travel in the form of a ellipsoid plume that has been predicted by both theory and experiments.

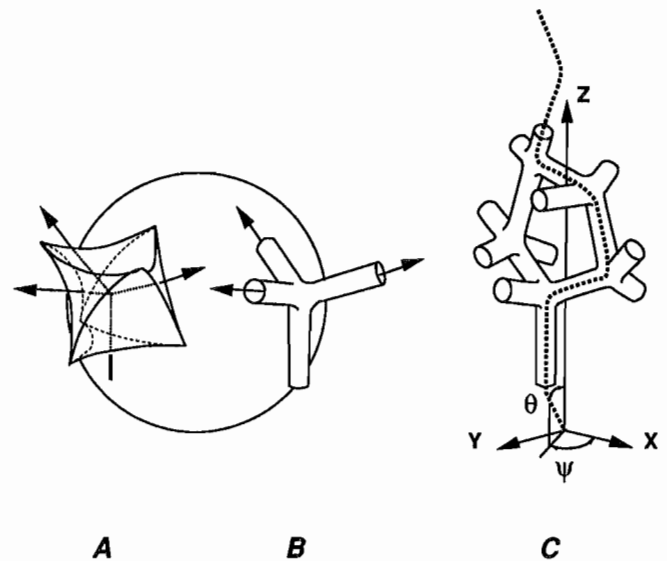


Figure 5.—Pore canal system. A, Tetrahedral pore between four spheres; B, pore schematized bifurcation; C, random path chosen by foreign particle through canal system (14).

The de Josselin de Jong model is a mathematical representation that incorporates Darcy's law, the tensor character of dispersivity and effective porosity, residence time of the particles, and the probability that a certain particle will take a particular path. It is assumed that the particles are conducted as though the rock fractures were infinite and continuous. The model also takes into account the changes in concentration of the plume as it disperses. The distribution of the particles is Gaussian as they flow within a fracture (12).

There are many advantages of applying this method to the problem of in situ leaching. By means of a tracer, information on effective porosity, changes in concentration, standard deviation, and mean travel time can be obtained to compute longitudinal and transverse dispersion if more than two fracture families exist. To implement this model, general knowledge of local flow characteristics is required. Dispersion can be observed in the field if one slug of tracer is released from an upgradient well and later detected in wells downgradient. The solutions to the problem are derived from the basic equation for transport of a solute in saturated porous media as described by Bear (3):

$$\frac{\partial c}{\partial t} = - \langle V_i \rangle \frac{\partial c}{\partial x_i} + D_{ij} \frac{\partial^2 c}{\partial x_i \partial x_j} - R_x, \quad (1)$$

where c = concentration (M/L^3),
 t = time (T),
 $\langle \rangle$ = mean value,

V_i = i th component of fluid velocity (L/T),

x_i, x_j = space coordinates (L),

D_{ij} = i, j component of the hydrodynamic dispersion tensor (L^2/T),

and R_x = rate of conversion or adsorption of solute (nonconservative tracer).

De Josselin de Jong (12) applied the theory of probability to this equation to describe the dispersion coefficients. The dispersion coefficients can now be related to N sets of continuous, equally spaced, and infinite fractures. The following equation shows the elements of the dispersion coefficient:

$$D_{ij} = \frac{1}{2\langle t \rangle} \left[\langle X_i X_j \rangle - \langle X_i t \rangle \frac{\langle X_j \rangle}{\langle t \rangle} - \langle X_j t \rangle \frac{\langle X_i \rangle}{\langle t \rangle} + \langle tt \rangle \frac{\langle X_i \rangle \langle X_j \rangle}{\langle t \rangle^2} \right], \quad (2)$$

where X_i, X_j, t = stochastic variables corresponding to the fracture system chosen,

$\langle X_i \rangle, \langle X_j \rangle$ = means of the displacement coordinates X_i, X_j ,

and $\langle X_i X_j \rangle, \langle X_i t \rangle, \langle X_j t \rangle, \langle tt \rangle$ = means of the products of the stochastic variables X_i, X_j , and t as combined between brackets $\langle \rangle$.

For the two-dimensional case, D_{ij} can be expressed as (13):

$$D_{ij} = \begin{bmatrix} D_{xx} & D_{xy} \\ D_{yx} & D_{yy} \end{bmatrix} = \begin{bmatrix} D_{11} & 0 \\ 0 & D_{22} \end{bmatrix}, \quad (3)$$

$$D_{xx} = \frac{1}{2\langle t \rangle} \left[\langle xx \rangle - 2\langle xt \rangle \frac{\langle x \rangle}{\langle t \rangle} + \langle tt \rangle \frac{\langle x \rangle^2}{\langle t \rangle^2} \right], \quad (4)$$

$$D_{xy} = D_{yx} = \frac{1}{2\langle t \rangle} \left[\langle xy \rangle - \langle xt \rangle \frac{\langle y \rangle}{\langle t \rangle} - \langle yt \rangle \frac{\langle x \rangle}{\langle t \rangle} + \langle tt \rangle \frac{\langle x \rangle \langle y \rangle}{\langle t \rangle^2} \right], \quad (5)$$

$$D_{yy} = \frac{1}{2\langle t \rangle} \left[\langle yy \rangle - 2\langle yt \rangle \frac{\langle y \rangle}{\langle t \rangle} + \langle tt \rangle \frac{\langle y \rangle^2}{\langle t \rangle^2} \right]. \quad (6)$$

The mean values in equations 4 to 6 are computed by summing the products of the stochastic variables and the corresponding probability of choice (g_m) if m sets of fractures are considered:

$$\begin{aligned} \langle x \rangle &= \sum_{m=1}^m x_m g_m \\ \langle y \rangle &= \sum_{m=1}^m y_m g_m \\ &\vdots \\ \langle tt \rangle &= \sum_{m=1}^m t g_m. \end{aligned} \quad (7)$$

The principal values, D_{11} and D_{22} , of the tensor D_{ij} are given by (12-13)

$$D_{11} = \frac{1}{2} (D_{xx} + D_{yy}) + \frac{1}{2} \sqrt{(D_{xx} - D_{yy})^2 + 4D_{xy}^2}, \quad (8)$$

$$D_{22} = \frac{1}{2} (D_{xx} + D_{yy}) - \frac{1}{2} \sqrt{(D_{xx} - D_{yy})^2 + 4D_{xy}^2}. \quad (9)$$

The angle, ψ , between the major principal axis, D_{11} , and the x -axis is given by equation 10 (12-13),

$$\tan \psi = \frac{2D_{xy}}{(D_{xx} - D_{yy}) + \sqrt{(D_{xx} - D_{yy})^2 + 4D_{xy}^2}}. \quad (10)$$

Dispersivity (α) is calculated as the dispersion coefficient divided by the velocity, or

$$\alpha_{11} = \frac{D_{11}}{\langle V \rangle}, \quad (11)$$

and

$$\alpha_{22} = \frac{D_{22}}{\langle V \rangle}, \quad (12)$$

where $\langle V \rangle$ = mean value of fluid velocity.

Way and McKee (45) solved de Josselin de Jong's theoretical dispersion equation for instantaneous contamination from a point source to obtain

$$C(x,y,t) = \frac{M}{\phi} \sqrt{\frac{1}{(4\pi D_L t)(4\pi D_T t)}} \exp \left[-\frac{1}{4D_L t} (x - v_x t)^2 - \frac{1}{4D_T t} (y - v_y t)^2 \right], \quad (13)$$

where C = concentration (M/L^3),

M = injected mass (M),

ϕ = porosity,

D_L = longitudinal dispersion coefficient (L^2/T),

D_T = transverse dispersion coefficient (L^2/T),

v_x, v_y = x and y components of the ground water velocity (L/T),

and t = time (T).

METHODS OF MEASURING FLOW CHARACTERISTICS OF FRACTURED MEDIA

The goal of this research is to find the rate of flow, the direction (x,y,z) of flow of the lixiviant, and the concentration of the plume at selected locations along the path of flow. In order to find the rate of flow, Darcy's law was applied to the fractured rock by assuming rock is an equivalent porous media. Darcy's law is given by

$$Q = -K A \frac{dh}{dl}, \quad (14)$$

where Q = volume flow rate (L^3/T),

K = hydraulic conductivity (L/T),

A = cross-sectional area of medium (L^2),

and dh/dl = hydraulic gradient.

The only difference is, for fractures, A , the cross-sectional area of the medium, is now represented as the cross-sectional area of the fractures assuming an impermeable rock matrix. It was assumed that the fracture is smooth walled and that its walls are parallel.

Solutions of the Navier-Stokes equation (43) show that steady, laminar flow through two smooth-walled parallel plates separated by a constant distance, $2b$, obeys the Cubic law (fig. 6) (46). The Cubic law is given by

$$Q = \frac{\gamma}{12\mu} (2b)^3 \frac{dh}{dl}, \quad (15)$$

where Q = volume flow rate per unit length of fracture (L^2/T),

γ = unit weight of fluid (M/LT^2),

μ = dynamic viscosity of fluid (M/LT),

dh/dl = hydraulic gradient,

and $2b$ = aperture of the fracture (L).

Therefore, in order to solve for Q , the hydraulic conductivity, hydraulic gradient, and/or the fracture aperture must be known. These values can be obtained by various means, such as air permeability tests, water permeability tests, or indirectly by measuring fracture apertures.

Permeability is a property of porous media and is a measure of the capacity of the medium to transport fluids and gases. Hydraulic conductivity is also a measure of the capacity of the medium to transport fluids and gases, but the properties of the fluid or gas (density and dynamic viscosity) are also taken into consideration. Because igneous and metamorphosed crystalline matrices have extremely low hydraulic conductivities, it is the fractures within the rock mass that influence permeability. Permeability can be measured with either gases or incompressible fluids. There is a difference, however, between measuring flows with either gas or liquid. When the size of openings in a medium approaches the mean free path of molecules, gases will flow through the medium more rapidly than would be predicted by Darcy's law. Laminar flow theory assumes zero fluid velocity at a solid fracture wall, with shear taking place within the fluid. The individual molecules in a gas, however, are in motion, and they contribute a velocity effect whenever the mean free path approaches

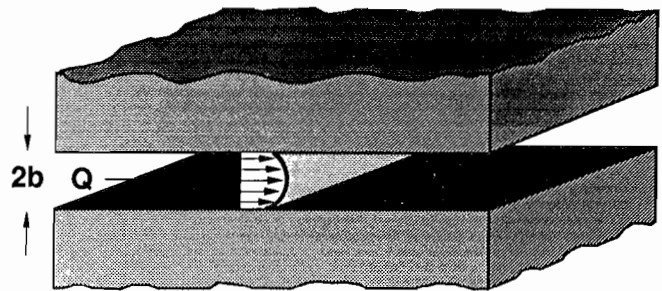


Figure 6.—Parallel plates illustrating Cubic law. Q = volume flow rate; $2b$ = aperture of fracture.

the dimensions of the flow conduit (26), therefore increasing the measured permeability. This is known as the Klinkenberg effect. This phenomenon could have exaggerated the results of the air tests.

Both compressed air and water packer tests were run for this study to determine fracture hydraulic conductivities. The advantages of using air are (1) air is much easier to work with, (2) there is good test repeatability, (3) the data are easier to evaluate, and (4) more tests can be run with respect to time. On the other hand, the disadvantages are (1) air "slips" because of the Klinkenberg effect, (2) air is not influenced by gravity, whereas water is, and (3) the data are probably more accurate in water tests with respect to applications of fluid lixiviants. Problems with the water tests are that (1) there is poor repeatability of the tests since it is not known whether the wetting front is being measured or if saturated fractures are being measured; because of this reason, permeability analysis using water requires saturated conditions prior to fluid injection, (2) a fairly clean water source is needed, (3) it is hard to wet all fractures in all tests to the same extent, and (4) air in the water lines is a common occurrence, giving false data. The purpose of this study was to describe the behavior of a fluid lixiviant, which water best represents.

METHODS OF ANALYSIS

An analytic solution to equation 1 was used to calculate the migration and concentration of the lixiviant in the ground water (23). Calculations were in two dimensions, and the fracture network was considered to be N sets of continuous, equally spaced, infinitely long fractures. The analytic solution was used to calculate the dispersion of a lixiviant in ground water as a function of time, distance, and direction from a source of a lixiviant. It is assumed that the ground water flow rate and direction do not change with spatial location. Other assumptions are that a uniform hydraulic gradient is present and that

fractures within each family (fractures with similar orientations) are continuous and equally spaced (25, 29).

In order to calculate dispersivities, D_{ij} , de Josselin de Jong's theory using equations 2 through 12 was solved. The following information was needed:

- directional components of ground water flow,
- hydraulic conductivity,
- direction of hydraulic conductivity,
- number of fracture families,
- fracture spacing of each fracture family,
- strike of fracture families,
- frequency of fracture family occurrence,
- standard deviation of the spacing of individual fracture segments, and
- average porosity of the fracture family.

The required information was obtained by detailed mapping of the mine drifts and raises adjacent to the study area, logging of core from wells to be used later for hydrologic testing, previous work done for the Office of Crystalline Rock Depositories (OCRD), and research done for nearby Superfund sites (7-8). Direction of ground water flow was assumed from the well data (6) and the strike and dip of the major mineral veins in the region (19). Because the direction of hydraulic conductivity was not known, a sensitivity analysis was performed using the analytic solution.

An equivalent porous media model using de Josselin de Jong's theory was used instead of a discrete fracture model. With the PLUME analytical model, many fracture sets may be superimposed. Discrete fracture models are limited to very few fracture sets (29). When mapping a large area, such as a mine, a large number of fracture sets can be identified, and all or some may play a major role in contaminant transport. The problem is in determining which fracture sets play a major role.

GEOLOGY OF EDGAR MINE SITE

HISTORICAL GEOLOGY

The Edgar Mine is located within the Colorado Front Range, an area that has been varyingly affected by seven tectonic and/or structural events dating back 1.75 billion years (22). The predominant rock types in the area consist of Precambrian metamorphosed sedimentary rocks (the Idaho Springs Formation), metamorphosed igneous rocks, and igneous rocks.

Three geologic events have played a major role in developing the structural trends present in the mine today.

1. The Precambrian sedimentary basement rocks were regionally metamorphosed through deep burial during the Boulder Creek Orogeny (1.75 to 1.69 billion years ago), which is also responsible for plastic deformation of these rocks into major folds with north-northeast trending axes. This deformation also was accompanied by intrusions of igneous rocks (19).

2. Another Precambrian deformation (1.3 billion years ago) followed. This event was predominantly cataclastic, with minor and local recrystallization and folding (22).

3. The structural framework established during the Precambrian Era strongly influenced major post-Precambrian events (19). During the Laramide Orogeny (70 to 40 million years ago), Precambrian-age fracture sets were reopened, and a younger set of fractures was superimposed on the older fractures throughout the region (22). These last two events resulted in brittle failure of rocks of the central Colorado Front Range.

The mine is located on the steeply dipping northwest flank of the Idaho Springs anticline. The anticline is asymmetric and trends approximately N55°E (a result of the second Precambrian deformation). Approximately one-fourth of a mile southwest of the mine is the Idaho Springs fault, which trends approximately N60°W in this region. Most of the faults in the area are Tertiary in age (2 to 12 million years ago) and generally follow preexisting planes of weakness in the Precambrian rocks (19).

SITE GEOLOGY

The geology of the site (the stope room and the vent shaft) is shown in figure 7. The predominant rock types include banded quartz biotite gneiss, granitic pegmatite, and biotite hornblende schist. The orientation of the schist zones often defines the foliation orientation because of the schist's relative structural weakness. Average attitudes of the foliation are N70°E with a dip of 75°NW. Gangue minerals include biotite, quartz, feldspars, hornblende, chlorite, and mostly pyrite, which is common in veinlets and is also found to be disseminated throughout the rock mass and on fracture surfaces.

A fault or shear zone has been mapped in the incline that leads to the stope site. This fault is not likely to affect the hydrology of the site because of its orientation. The most common joint sets in the stope area have been measured to be N50°E/32°SE, N50°E/50°NW, and S75°E/41°SW.

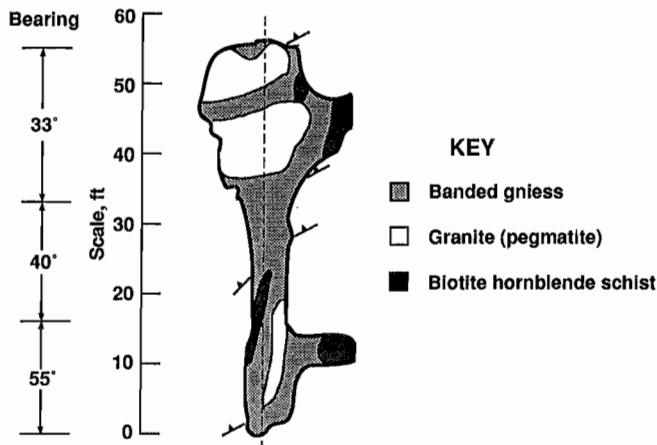


Figure 7.—Geology of experimental stope site.

LOCAL HYDROLOGY

Ground water in the Idaho Springs area is primarily found in fractured igneous and metamorphic rock aquifers. Porosities of the regional rock matrices have been measured to be extremely low: 4×10^{-1} to 1×10^{-4} (9) and 1×10^{-2} to 1×10^{-3} (24). Fracture porosities in similar crystalline rocks in Colorado range from 1 to 4×10^{-3} for depths of 20 m and 2 to 4×10^{-6} for depths of 50 to 200 m (39, 41). When considering porosities of the entire rock mass, the mine workings increase the total porosity. The hydraulic conductivity of the rocks in the Edgar Mine has been found to range from 2.8×10^{-6} ft/d to 2.8×10^2 ft/d (32). Snow (41) found regional hydraulic conductivities to range between 0.01 ft/d and just over 1 ft/d. The water packer tests performed for this study showed hydraulic conductivities to range between 3.0×10^{-2} ft/d and 1.16×10^1 ft/d; however, there was one anomalous hydraulic conductivity of 2.61×10^3 ft/d.

Fractured aquifers in the area have been estimated to be between 200 and 350 ft in depth (15, 40). Because fracture density in these types of aquifers decreases with depth, it is believed that greater than 90% of the Idaho Springs aquifer hydraulic conductivity is within 80 ft of the surface (7). The regional water table is located between 150 and 200 ft below the ground surface (30) and between 50 and 175 ft where the topography is gently sloping (30). However, the regional water table has been artificially lowered within the past 100 years because of mine workings that provide deep drainage. In addition, this water table rises and falls considerably with climatic variations. As such, modeling lixiviant flow in such an extensively mined area may not be very conclusive.

Locally, the hydraulic gradient seems to be controlled by the regional structural geology, rather than the topography. Wells on the Edgar property, which were installed by the U.S. Army Corps of Engineers, show that the potentiometric surface in the wells parallels the majority of the attitudes of joints, measured adjacent to the wells (6).

HYDROGEOLOGY OF EDGAR MINE

Today the Edgar Mine is considered to be dry. This was not so when the mine began operation in about the mid-1860's. Construction on the Miami Tunnel, currently the main portal into the mine, began around 1870. The purpose of the tunnel was to provide easier haulage from lower workings and drainage for the mine. In the early 1900's the Big Five or Central Tunnel was driven at the west end of Idaho Springs. This new haulage and drainage tunnel intersected the same workings as the Miami Tunnel, but at greater depths, and provided a lower drainage

for the workings; thus the Edgar Mine was no longer considered a wet mine.

The mine is not entirely dry. The first 100 ft or so into the mine is occupied by a highly permeable zone that is due to a large amount of fractures caused by freeze-thaw weathering and stress relief. This zone responds to seasonal changes in precipitation, leaving most of the rock matrix in the zone saturated year round (31).

RESEARCH DESIGN AND IMPLEMENTATION

Obtaining the critical hydrologic information concerning the rock mass involved several steps. The first step after obtaining any published geologic, geophysical, and hydrologic data was to map the geology and structure of the research site and drifts adjacent to the site. Core from the eight test wells (fig. 3) at the site also supplied much-needed geologic information. The fractures in the mine and core were studied carefully to determine which ones were likely to conduct fluids and in which direction. Packer tests were conducted to determine the hydraulic conductivity of fluids within the fracture networks.

METHODS

Although mapping surface fractures and geology exposed in the mine ribs, roof, and floor was a useful method for characterizing the rock mass, more information was needed concerning the rock mass characteristics. Fractures exposed in the mine drifts may have been the result of blasting; therefore, wells were drilled to examine the nature of fractures in undisturbed rock.

Geologic Mapping

Mapping of the geology and structures in the mine drifts was conducted using a Brunton compass. A total of 1,146 linear feet of drifts adjacent to the site were mapped to identify lithological and structural discontinuities. The stope room was mapped in more detail than the surrounding area, at 1-ft intervals instead of 5-ft intervals (fig. 7). Additional information on geology was obtained from logging core from wells 6 and 8 drilled at the site. This core was not logged for fracture information.

Well Field Design

A well field of five wells was installed to obtain both geologic and hydrologic data (fig. 3). Three additional wells were drilled in the drift below the proposed stope, but these wells were intended for monitoring purposes in the future. Because of the small size of the stope room,

Beyond 100 ft, the mine is generally dry. There are areas, however, near the stope site that also exhibit a response to precipitation. The intersection of C-Right and C-Right Spur (fig. 3) is one such area. The mine also tends to get wetter toward the Edgar vein where the Miami Tunnel ends. The stope site is located in a presently dry site that housed the mine's reservoir until 1988.

and limited access to certain areas via drifts, wells 1 through 4 were configured to have a close spacing between wells, with a 120° angle between wells 2, 3, and 4 (fig. 3). This configuration was used to determine if directional permeability existed. Well 5, drilled at an angle of 45°, showed that there were very few vertical fractures in the area of the stope. In addition, the data from well 5 did not show a new fracture orientation different from that found in wells 1 through 4. Wells 6, 7, and 8 were drilled below the future stope. Well 7 was logged to determine if fracture orientations were different from those of the other logged wells.

Drilling and Core Recovery

A CP-65 drill rig was used to diamond drill each well. Wells for the hydrologic study (wells 1, 2, 3, 4, and 5) along with well 7 were 4 inches in diameter. Wells 6 and 8, intended to be used only for monitoring purposes, were 3 inches in diameter. Although core was recovered from wells 6 and 8, it was not logged for fracture information, because there were no hydrologic tests planned for D-Right drift. Core was logged on-site for general geologic description and recovery. It was then boxed and transported to a laboratory at the Bureau in Denver, so it could be logged in more detail.

The core from each of the 4-in wells was oriented using a simple but effective (accurate to $\pm 10^\circ$ strike) method, which consisted of the following steps:

- Plasticized clay was inserted into an aluminum cup that was welded to the end of aluminum rods (fig. 8).
- While the rod was oriented to the north, the assembly was lowered into the well.
- An impression was taken at several 5-ft intervals in each well.
- The impression was matched to the top of the core taken from the next run.
- A north mark was made on each run of core from the north mark on the matching imprint.

Core Logging

The core from each well was logged primarily for information on fractures, but information also included the petrology and mineralogy of the core and other pertinent data. A total of about 200 ft of core was logged. One hundred and twenty feet came from the four vertical wells (wells 1, 2, 3, and 4) and 80 ft came from wells 5 and 7, which were inclined at approximately a 45° angle.

For logging, the core from each well was laid out, and each length of core was matched to the next length. When lengths of core would not fit together (mostly because of drilling damage), foliation trends would be used to approximate the in situ position of the core. Next, each length of core was etched with a mark indicating north. Each length of core was carefully examined for fractures located on the ends of each piece of core or sealed fractures found within each piece of core. A goniometer (fig. 9) was designed and built to measure the dip of each fracture, and by using

the etched north mark on the core, the strike of the fracture.

The information gathered on each fracture was compiled on log sheets. The information included depth of fracture, type of fracture, strike and dip, fracture characteristics, rock type, and rock quality designation (RQD).

After the core data were compiled, an attempt was made to see if there was a recognizable pattern or preferred direction of the fractures. The majority of the fractures logged from the core were oriented with a dip direction ranging from N70° to 80°E and around due north with a dip ranging from 30° to 40°NW. This is not consistent with the fracture orientations found in the mine (fig. 10). Fractures with notable oxidation or mineralization were inspected for a preferred orientation, but a preferred orientation was not found. Figure 11 shows the effects of blasting on fracturing. The development of the D-Right drift caused extensive fracturing in nearby rock, reflected in well 3.

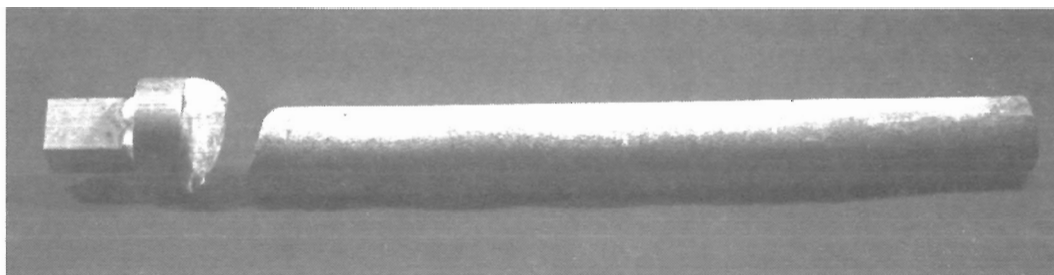


Figure 8.—Core orientor.

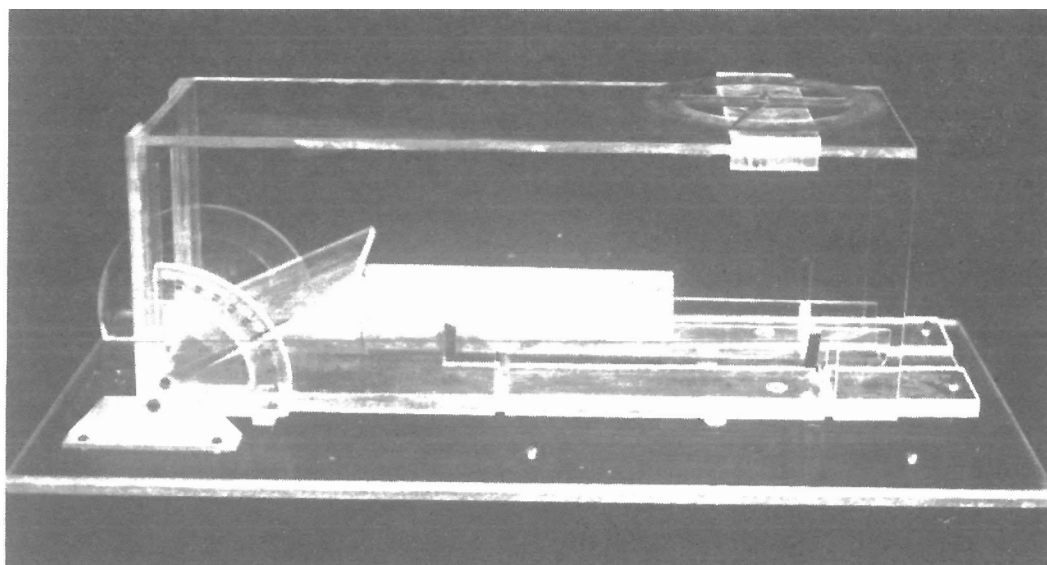


Figure 9.—Goniometer.

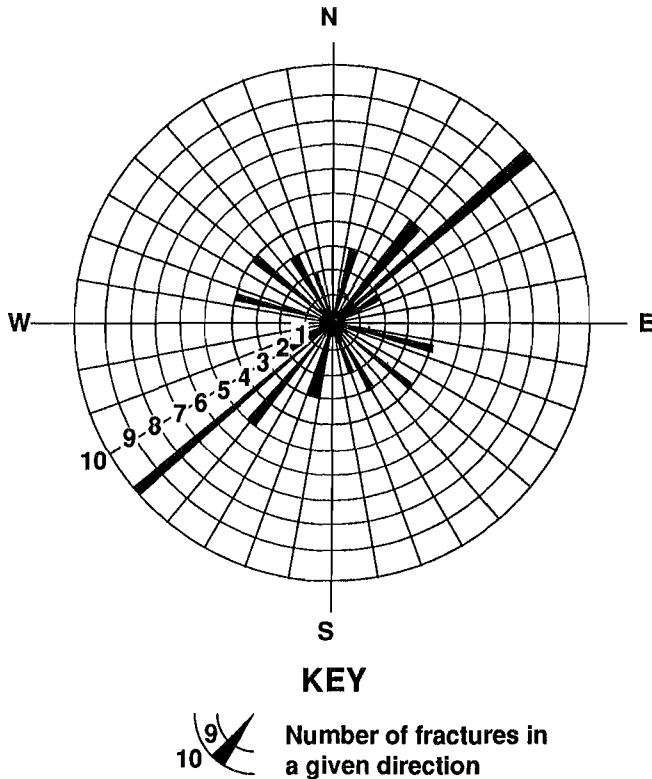


Figure 10.—Rose diagram of core fracture dip orientations from test wells.

Overall Geologic Interpretation and Analysis

Joint and fracture characteristics, such as orientation, spacing, trace length, aperture, and hydraulic conductivity, are very crucial to accurately model transport of contaminants through a crystalline rock mass. There are several problems associated with the data collected for this study. Data are limited because of time constraints, and access to the rock mass was only possible from the surface, drift, or core logging. The data are also biased toward the more visible and predominant fractures. If the data are used in models to describe the entire rock mass, the sample can only be considered a representation of the trends of the rock mass. Since the collected data represent a small fraction of the rock mass characteristics of interest, statistical analysis was used to obtain maximum information from these limited data.

The data sets for this analysis were obtained from mapping drifts adjacent to and including the stope area, well core logging in the stope area, and mapping and hydrological data collected by Montazer (31). The data were divided into several categories: orientation—obtained from core, drift mapping, and Montazer's dissertation; spacing—obtained also from core and drift mapping; trace length—observed from drift mapping; aperture—measured by Montazer in bore holes in the Office of Nuclear Waste

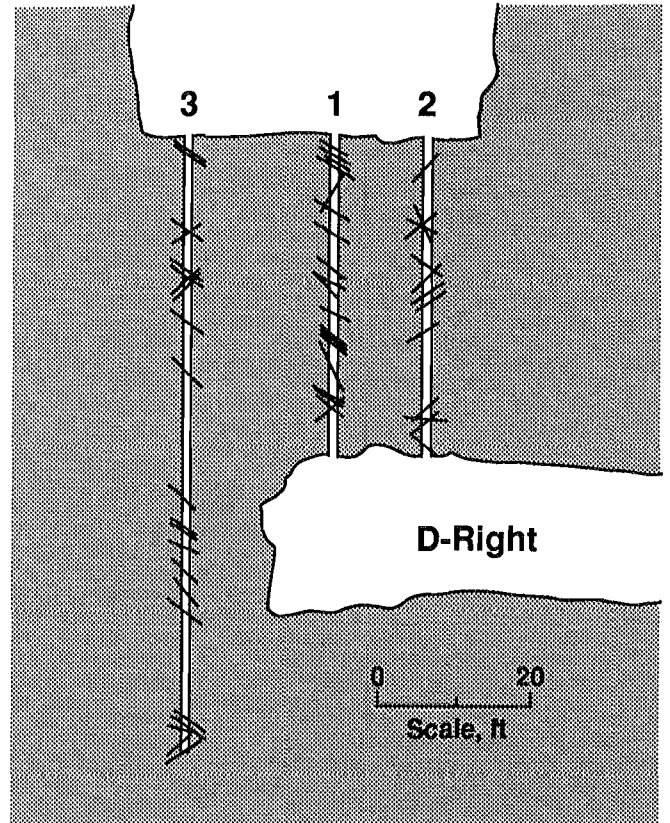


Figure 11.—Blast damage from D-Right drift. Numbers indicate wells.

Isolation (ONWI) room; and hydraulic conductivity—obtained by Montazer from packer tests in wells and packer tests performed by the Bureau at the stope site.

The cumulative probability of each fracture data set, such as orientation, spacing, length, aperture, and hydraulic conductivity, was calculated and then plotted on several different types of probability paper to find the best probability distribution of the data. Figures 12A through C show that fracture orientations (strike) fit a normal probability distribution function,

$$F(x) = \frac{1}{\nu(2\lambda)^{0.5}} \int_{-\infty}^x \exp\left[-\frac{(x-\mu)^2}{2\nu^2}\right] dx, \quad (16)$$

since this function plots as a straight line on normal probability graph paper. The strike data for figure 12A were collected from wells 1, 2, and 3 located in the stope room. This data set represents all of the logged fractures in a total 80 ft of core. Figure 12B represents drift mapping of fractures. A bias associated with mapping fractures was encountered in logging the core and mapping drifts since the chance of intersection between the fractures and the sampling area decreases as the angle

between the two decreases (28). This bias is fairly strong with respect to the wells as compared with the drifts, where a larger opening gives more information. On the

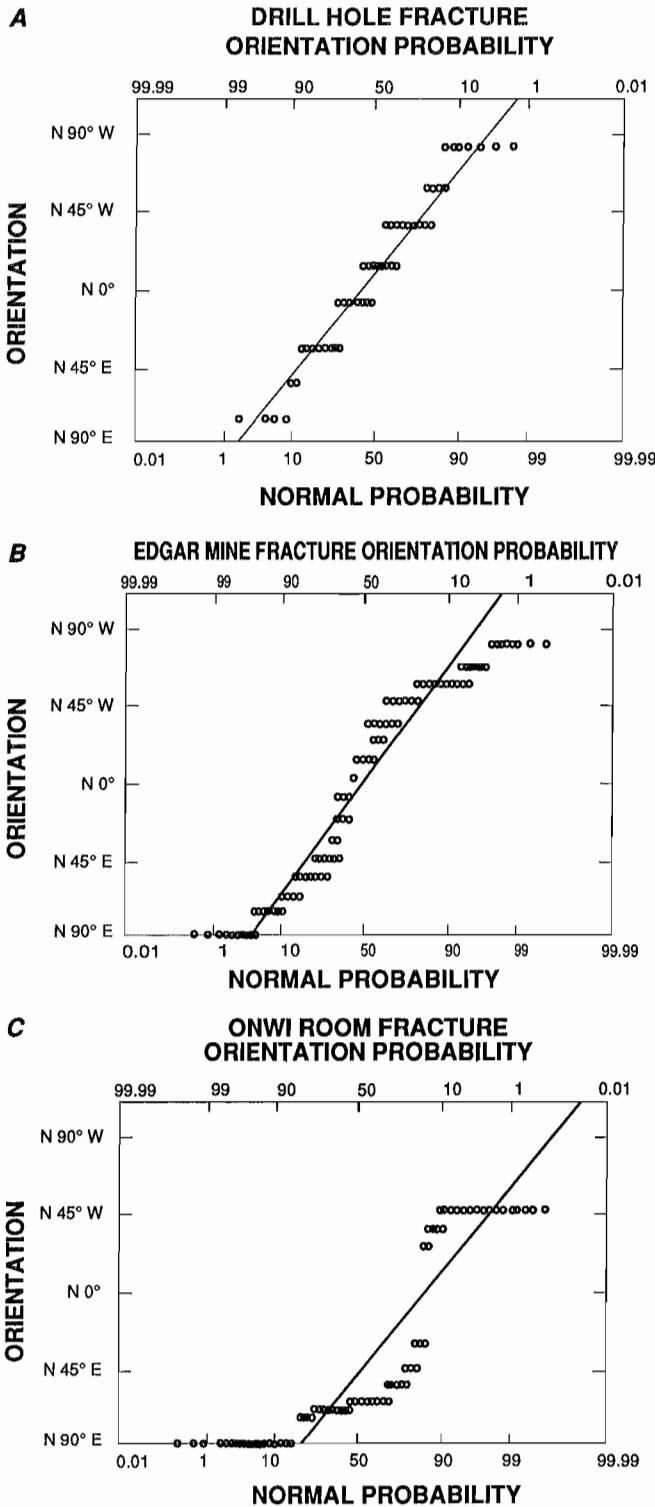


Figure 12.—Probability distribution of fracture orientations from (A) test wells, (B) mine drifts, and (C) research by Office of Crystalline Rock Depositories. ONWI = Office of Nuclear Waste Isolation.

other hand, all encountered fractures were noted in logging, but only the most developed fractures were noted when mapping the drifts. Figures 12A and B show a better fit to the normal distribution than figure 12C. There are several ideas as to why the third data set appears to differ. The data for figures 12A and B were collected approximately 1,200 to 1,600 ft into the mountain, and the data for figure 12C were collected approximately 700 ft into the mountain by different researchers. Mapping techniques could have differed between the two groups. Also, since the data for figure 12C are from a location closer to the surface, other fracturing mechanisms, such as stress differences, could have affected this location. However, the data in figure 12C are typical of the region (22, 30).

Figure 13 shows that spacing between fractures follows a log-normal probability distribution. This same distribution has been found in other investigations of fracture and joint spacing (2, 4, 32, 37, 42). Others suggest the distribution is negative exponential (1, 5, 14, 33, 40, 44). Snow (40), however, found the Poisson distribution to fit fracture data. At the Edgar Mine, the three-parameter log-normal distribution function, where β is the third-parameter boundary,

$$f(x) = \frac{1}{(x - \beta)\nu_n(2\lambda)^5} \exp \left[-\frac{(\ln(x - \beta) - \mu_n)^2}{2\nu_n^2} \right], \quad (17)$$

appears to have a much better fit than the two-parameter normal probability distribution for aperture. These two characteristics are closely related by the equation for log-normal distribution, where $(x - \beta)$ is replaced by x .

In mapping the spacing in both the core and drifts, only the apparent spacing was noted, meaning the strike and dip were not taken into consideration (fig. 14).

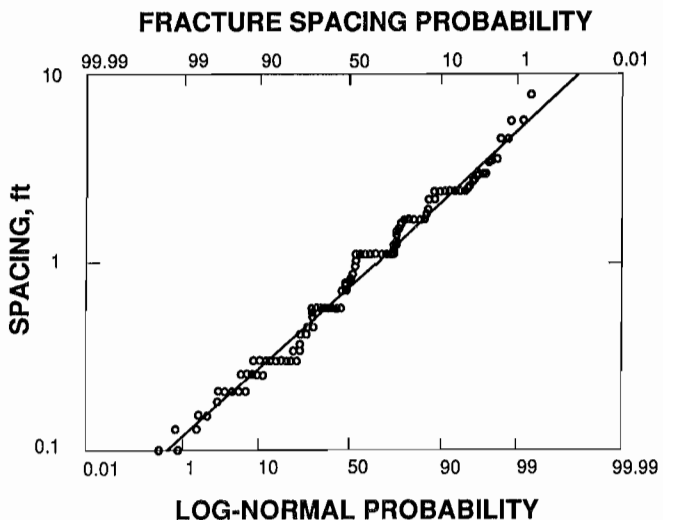


Figure 13.—Probability distribution of fracture spacing in mine.

Trace length (fig. 15) also follows a three-parameter log-normal probability distribution. Other studies also suggest the log-normal distribution for this characteristic (1-2, 4, 14). The negative exponential distribution was also found to fit data (5, 10, 33, 35).

Trace length is an important characteristic for modeling fracture flow. It is assumed that the longer the fracture, the better the chance of the fractures intersecting that fracture. The fracture lengths in the data set, however, are only the observable lengths, because it is impossible to measure the full length of the fracture since it may extend out of the field of vision (27). Figures 16, 17, and 18 show that the distributions of aperture and hydraulic conductivity, respectively, follow a two-parameter log-normal probability distribution, although the fit is not very accurate. Paschis (32) found that their data best fit a three-parameter log-normal probability distribution for aperture. These two characteristics are closely related by

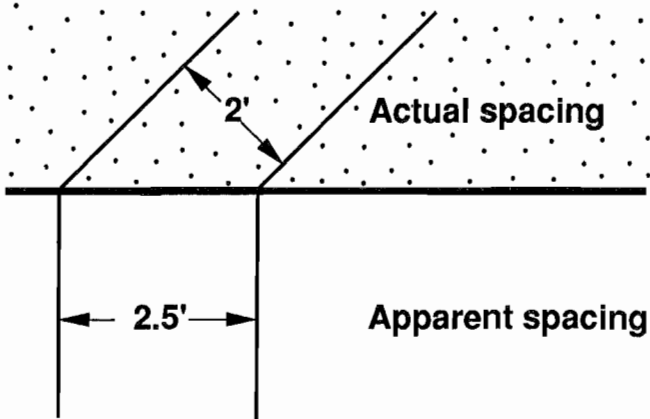


Figure 14.—Apparent spacing versus actual spacing.

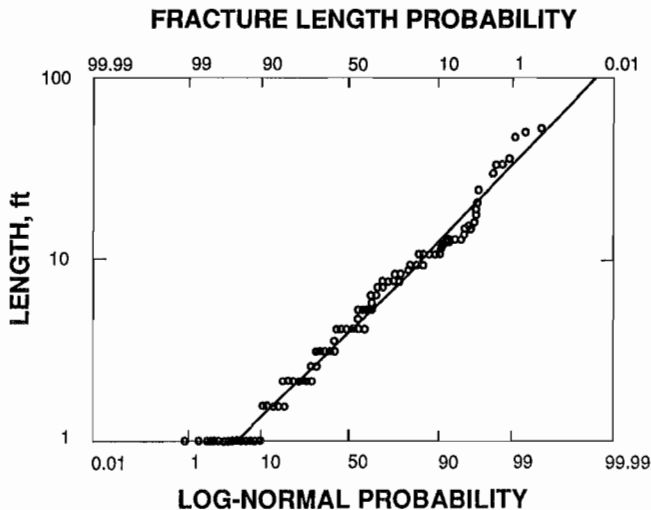


Figure 15.—Probability distribution of fracture trace length.

the equation for hydraulic conductivity for a fractured medium (46),

$$K = \frac{\gamma}{12\mu} (2b)^2, \quad (18)$$

- where K = hydraulic conductivity,
- γ = unit weight of water,
- μ = dynamic viscosity of water,
- and $2b$ = fracture aperture.

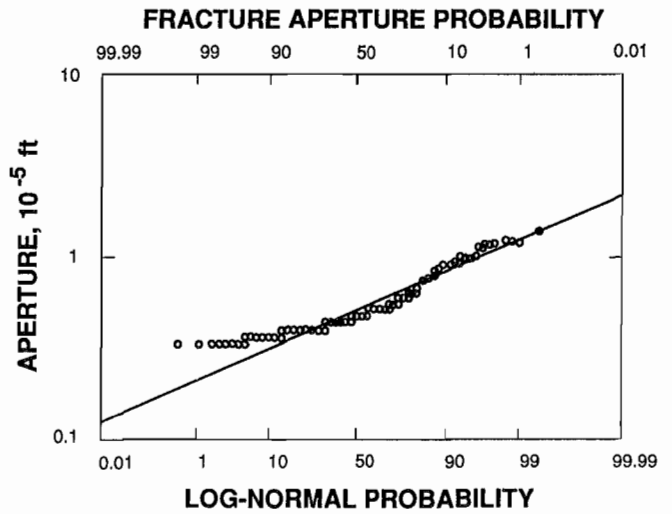


Figure 16.—Probability distribution of fracture aperture from research by Office of Crystalline Rock Depositories.

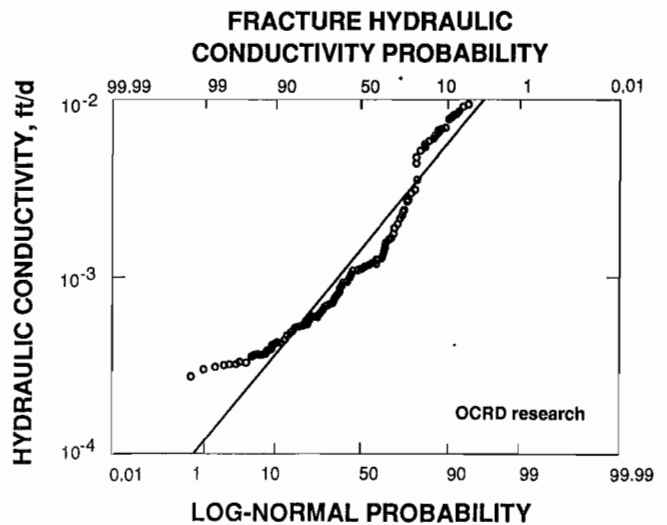


Figure 17.—Probability distribution of fracture hydraulic conductivities from research by Office of Crystalline Rock Depositories (OCRD).

The data used for these two characteristics were those that Montazer (31) obtained for his dissertation and from packer tests conducted at the stope site. These characteristics are very difficult to measure accurately. The aperture was measured inside Montazer's wells; therefore, the width of the fractures could have been damaged by drilling. Also, only the apparent width was measured.

Although the data collected for hydrologic modeling at the Edgar Mine may seem to be deficient, mathematical statistics show that the data do have a preferred distribution. This distribution shows that the data are non-random, and fairly accurate assumptions can be made as to whether to use certain data in modeling. Sampling errors may be present because of the data collection techniques. Understanding the nature of the errors and biases is important when utilizing these data in a hydrologic model, since the end result from the model may have to be modified.

Besides conducting the probability analysis, other ways to represent the data were used. Schmidt nets were used to find major trends in the fracture orientation data (fig. 19). Unfortunately, scatter in the plotted poles precluded giving the trend of the data. Because so much scatter was found, the data were questioned, and the probability analysis was conducted to see if the data were random.

Preferential fracture directions were found from plotting the strike of each measured fracture from the core, and drift mapping data on rose diagrams. The most common strike directions were found to be N80°E, 0°, and N70°E from the core, and S60°E and S30°E from the drift mapping. It could be assumed that fluid flow would be the greatest in the directions found to have the most common

strike. This may not be so in some cases, however, since the most common fractures may not have a high amount of connectivity, while the least common fractures may have the most.

It was found that at the stope site, the computer-generated dispersivities and their directions coincided with the preferred fracture directions (fig. 20). This agreement shows that the most common fractures have connectivity in the direction of dispersivity.

Hydrologic Testing

In order to assess the in situ hydraulic conductivity of fractures intercepted by the five wells, packer tests, using transient pressure decay techniques, were performed using both air and water. The equipment setup and procedures were similar for each test (figs. 21 and 22). Compressed air was used to inflate a set of packers that were used to isolate fracture zones for testing. In the air tests, compressed air was used to pressurize the packer annulus to 30 psi for approximately 2 min; then the decay of air pressure versus time was recorded. In the water tests, water was injected into the packer annulus, and the decay of the head of the water versus time was recorded.

These types of tests are similar to a slug test, in which a slug (a volume) of fluid is either instantaneously injected into or withdrawn from a well. The change in fluid level or pressure is then measured against time and matched to type curves in order to determine the in situ hydraulic conductivity in a single well.

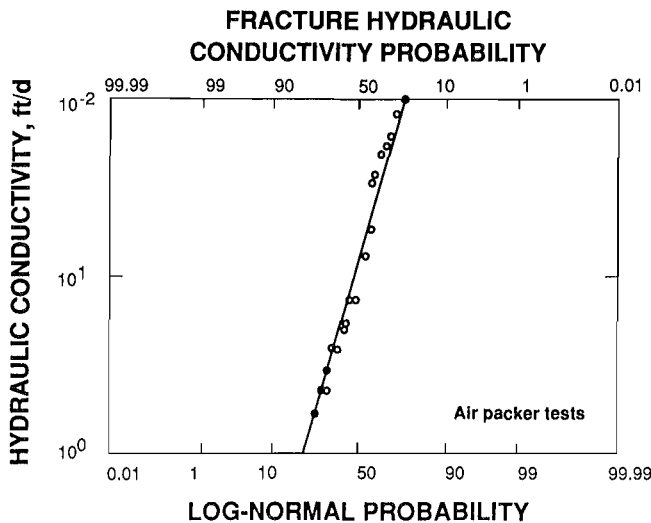


Figure 18.—Probability distribution of fracture hydraulic conductivities from air packer tests.

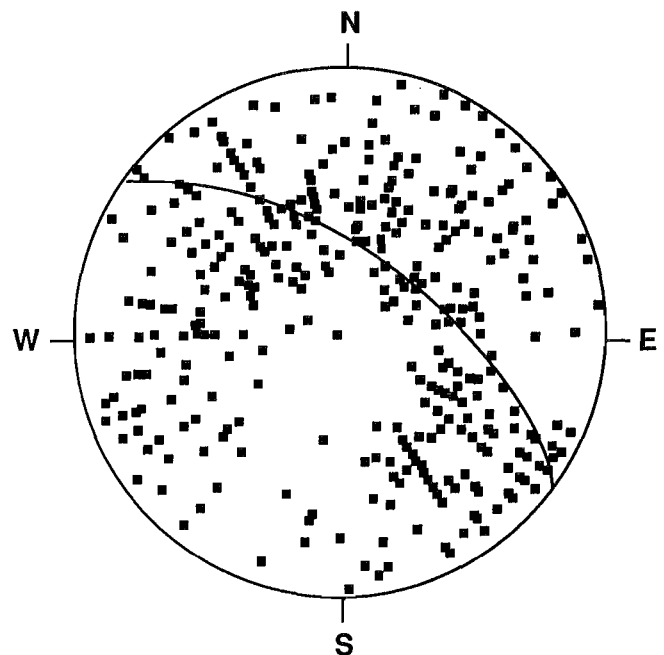


Figure 19.—Schmidt net from Edgar Mine fracture data.

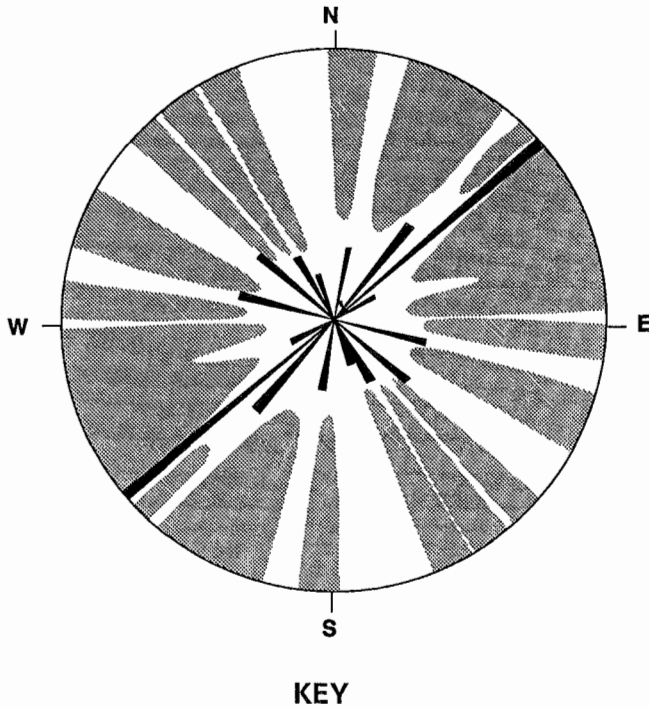


Figure 20.—PLUME model dispersivities versus rose diagram for slope site fracture dip orientations.

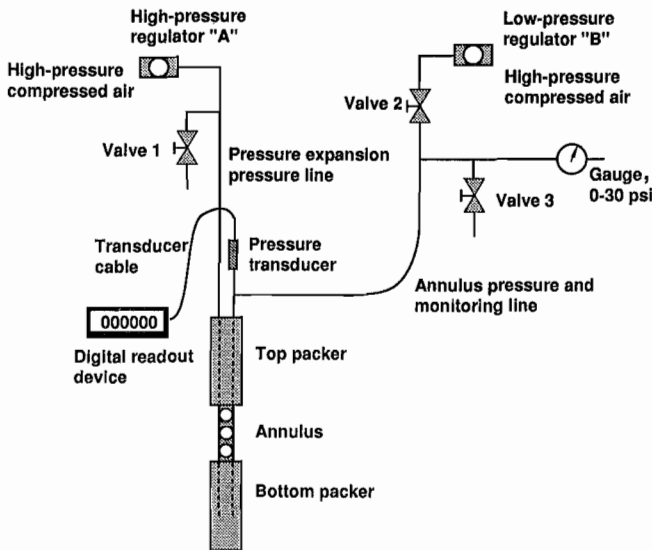


Figure 21.—Equipment setup for air packer tests.

The data collected from each packer test were plotted on semi-log paper (fig. 23). Each pressure data point was then divided by the initial pressure for that test to obtain a curve for matching to the slug test type curves (figs. 24 and 25). From the curve matching, the transmissivity, T,

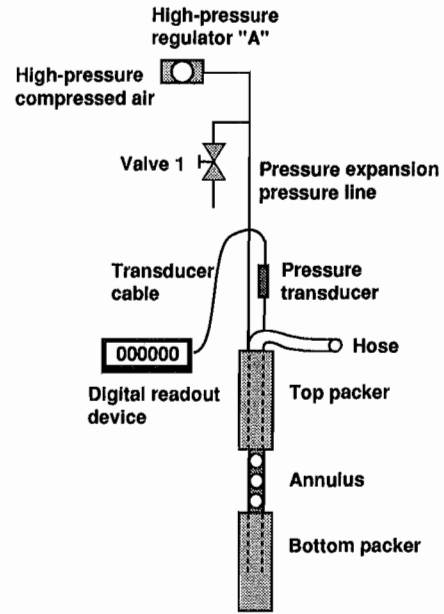


Figure 22.—Equipment setup for water packer tests.

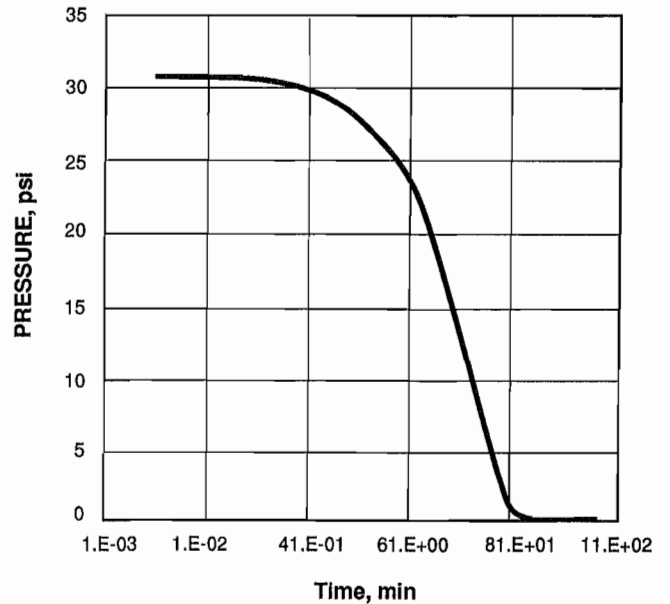


Figure 23.—Example of raw data from air packer test.

and hydraulic conductivity, K, for a fracture or set of fractures could be determined. The following equations were used to calculate hydraulic conductivity of the fractures (see figure 26 for an example of the matching procedure):

$$T = 604.41 \left(\frac{\alpha}{2u} \right) \frac{r^2}{t}, \quad (19)$$

$$\text{skin} = \frac{1}{2} \ln \left[2\alpha \left(\frac{e^{-2s}}{2\alpha} \right) \right], \quad (20)$$

$$2.31s = \rho ch, \quad (21)$$

where $e^{2s}/2\alpha$ = value for matched curve,

h = distance between packers (L),

K = hydraulic conductivity (L/T),

r = radius of well (L),

t = time at match line (T),

T = transmissivity (L²/T),

$\alpha = s = \text{skin factor}$,

$\alpha/2u = Tt/r^2 = \text{value at matched line}$,

and $\rho c = \text{porosity} - \text{compressibility product}$
 ((M/L²)⁻¹).

This matching and calculation procedure was done for all 37 of the intervals tested. Air permeabilities ranged between 0.16 and 1,200 ft/d. To calculate the equivalent hydraulic conductivity of the fractures from the specific or intrinsic permeability obtained in the air tests, the densities and viscosities of water and air were considered. Conversion of the air permeability data to equivalent hydraulic

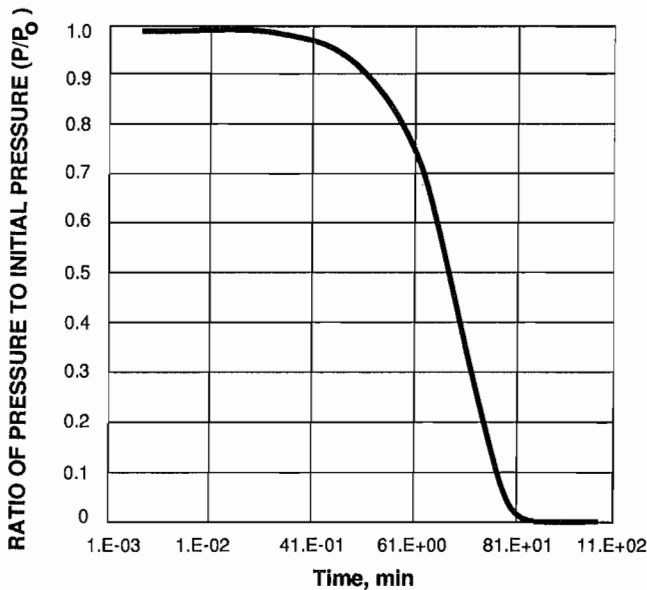


Figure 24.—Example of data to be used for curve matching.

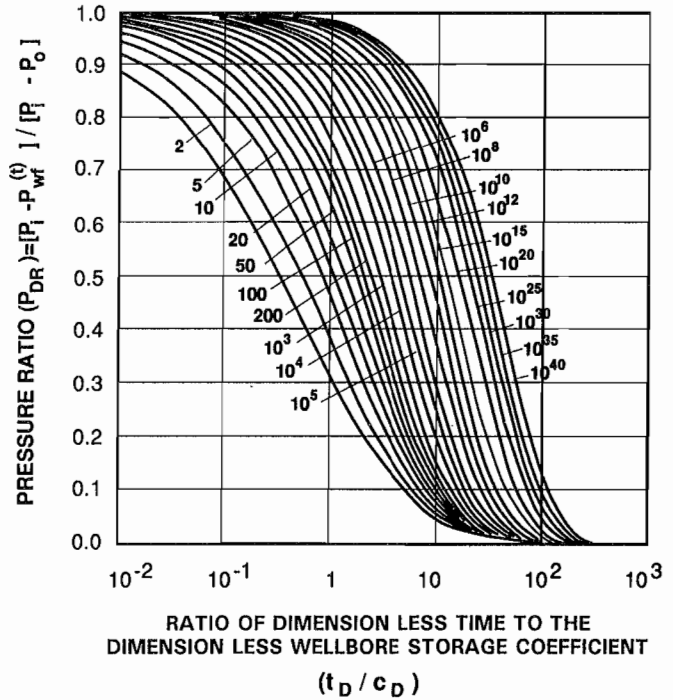


Figure 25.—Type curves for drill stem tests or slug tests (34).

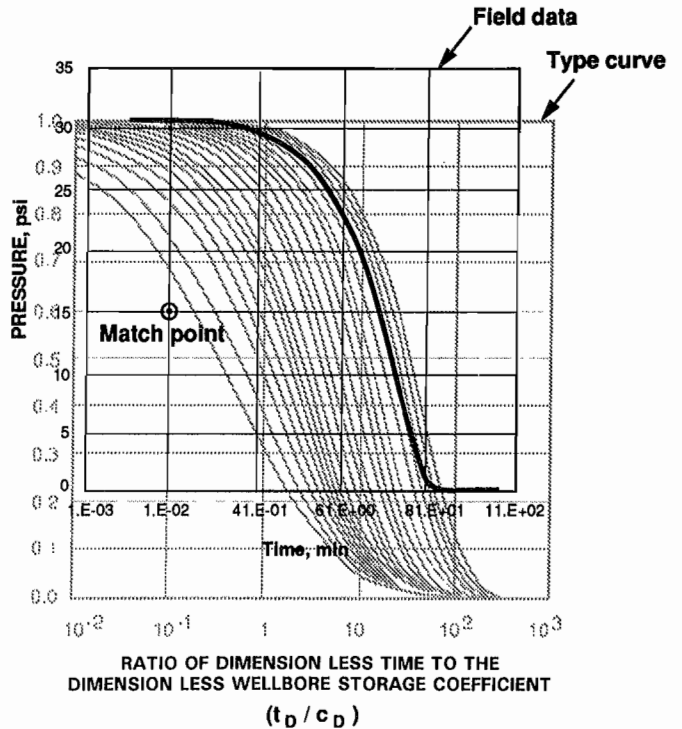


Figure 26.—Curve matching example.

conductivity produced values ranging between 2 and 15,000 ft/d. For water, the hydraulic conductivity range was between 0.03 and 2,610 ft/d. Tables 1 and 2 summarize the results from each type of test. Although different intervals were tested with the air and water, some fracture groupings were similar in both tests and a large difference in permeability magnitude could be observed. This magnitude of difference may be due to the Klinkenberg effect explained earlier or to the fact that water is affected by gravity more than air is. Another reason for air's high hydraulic conductivities is that the air had more avenues of escape as illustrated in figure 27. At times, the measured hydraulic conductivities for air were extremely high, most likely because of a direct path between the tested fracture(s) and a fracture exposed at the rock surface. The comparison of the tests shows that the water tests are the most accurate even though water is more difficult to work with. However, air permeability tests provide a rough but high range with less time and effort.

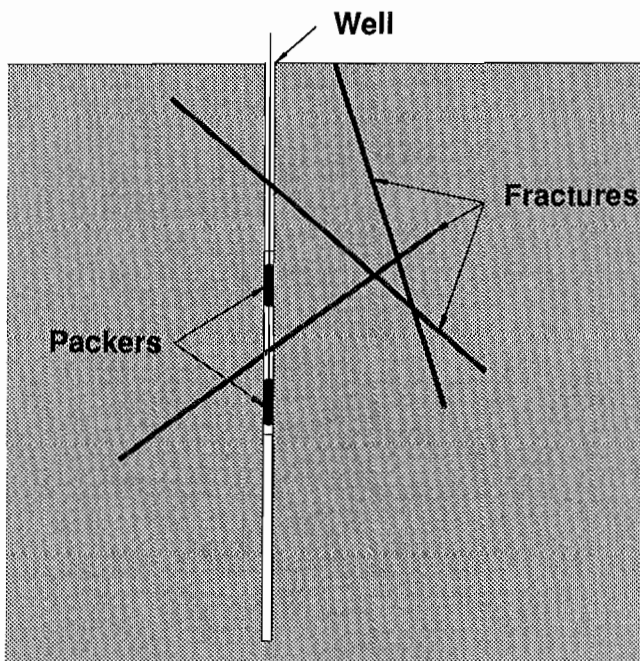


Figure 27.—Avenues of air loss during air packer tests.

Table 1.—Hydraulic conductivities from water packer tests

Fractures	Conductivity, ft/d	Fractures	Conductivity, ft/d
Well 1:		Well 4—	
678	Continued:	
6	3.40	7	0.10
6	2,610	Mean ...	5.20
Mean ...	8.73	Well 5:	
Well 2:		403
403	307
4	2.69	3	1.12
Mean ...	1.36	3	1.38
Well 3:		3	2.39
4	2.69	Mean ...	1.23
Well 4:		Summary:	
16	10.1	High	2,610
16	11.6	Low03
15	4.03	Mean ...	166
716	Median ...	1.89

Table 2.—Hydraulic conductivities from air packer tests

Fractures	Conductivity, ft/d	Fractures	Conductivity, ft/d
Well 1:		Well 3—	
2	28	Continued:	
6	110	7	2.0
6	160	8	75
7	7.3	9	63
8	64	10	44
8	230	Mean ...	670
8	510	Entire well ..	94
Mean ...	160	Well 4:	
Well 2:		6	4.7
1	7.8	7	3.6
2	34	7	4.2
3	83	7	2,200
4	110	7	2,400
Mean ...	59	8	2,300
Well 3:		8	15,000
2	20	9	2,100
3	3,300	15	2,000
4	2.3	Mean ...	2,900
4	3.6	Well 5:	
4	9.0	4	380
4	23	5	8.5
4	1,100	Mean ...	190
4	1,300	Entire well ..	8.3
4	3,800	Summary:	
5	140	High	15,000
5	650	Low	2.0
5	730	Mean ...	1,100
6	310	Median ...	110
6	450		

FRACTURE FLOW MODEL AND DATA ANALYSIS

The purpose of this research was to characterize and model the fracture hydrology adjacent to an underground mine stope. After compilation, the data were utilized for characterization, modeling, and sensitivity of plume migration to rock mass properties. The data were analyzed and sorted so trends and patterns could be observed. Then the data were applied to the PLUME model. The model calculated the general characteristics of lixiviant plumes that may be generated by in situ leaching at the Edgar Mine. The plots of the plumes were considered within the context of the local and regional hydrology to predict the behavior of a lixiviant plume traveling through the rock mass.

The analysis of flow was conducted using the PLUME model (equation 1). Peak concentration, measured at the intersection of the longitudinal and transverse plume axes, leaving the stope site was thought to be the most critical output of the model, besides the direction of lixiviant flow. Many of the data used for input into the model were approximated or measured from a small sample of rock mass. Therefore, a sensitivity analysis was used to determine the relationship of concentration to selected input variables.

Available data were input into the model. These included the initial mass of the lixiviant (41,639 g); average measured hydraulic conductivity (2.7 ft/d); the number of major fracture families in close proximity to the leaching site (15); the orientation of each fracture family, i.e., the direction the fracture is dipping, since flow would mostly occur in the direction of dip and not strike; location of the point source (0,0, the center of the plot); size of the area of interest (8,000 by 8,000 ft); fracture family spacing of the most predominant fracture family (1 ft); frequency of each fracture family (ranging from 1 to 8); saturated aquifer thickness (27 ft, the total depth of the stope); ground water velocity (0.27 ft/d) based on a gradient of 10^{-2} , which is within the range commonly observed in field situations (19); specific density of the rock mass (2.65); type of source (instantaneous); and the time period over which calculations are to be made (1 year for the sensitivity analysis).

Estimates were made on the following properties: porosity of the fracture openings (10% due to filling); standard deviation of frequencies (0.0, assuming fracture families are evenly spaced); and the direction of the hydraulic conductivity ($N6^{\circ}W$). Because the angle of ground water flow was not known and could not be estimated, a sensitivity analysis was performed to see which plume directions were possible given the known data. This was done by inputting ground water flow directions every 5° for 360° . When all of the generated data were compiled, possible plume directions were found to be flowing between $N76^{\circ}E$ and $S59^{\circ}E$ and $N59^{\circ}W$ and $S76^{\circ}W$

(fig. 28). The westerly direction is more probable, since the Big Five drainage tunnel lies to the west of the stope. The model results show the movement of the plume as it travels in a solely fractured rock mass, but when the plume is in close proximity to a major discontinuity, such as a fault, vein, or mine working, minor fractures will direct the flow toward that opening because of pressure differences.

Using the hydrologic data collected at the site, the model predicted flow in a westerly direction. Assuming all of the lixiviant escaped, the concentration of the plume would decline from an initial concentration of 150 ppm to 0.24 ppm after 1 year, after traveling about 100 ft from the site for the flow direction range in figure 28. By the time a lixiviant plume would reach the Big Five Tunnel, which is approximately 2,000 ft from the site, its peak concentration would be around 0.01 ppm (fig. 29). However, this prediction could be considered as a worst case scenario, since many of the values used in this run were critical to high concentrations. The best estimate of the lixiviant peak concentration at the Big Five Tunnel would be much less than 0.01 ppm based on this worst case scenario. Most likely, the concentration would be negligible, since the plume would be affected by field conditions, such as veins and mine workings, which were never considered in the model.

The sensitivity analysis of the plume characteristics showed that the dispersivity, ground water velocity, fracture porosity, and fracture spacing had notable effects on peak lixiviant concentration. Dispersivity was found to be

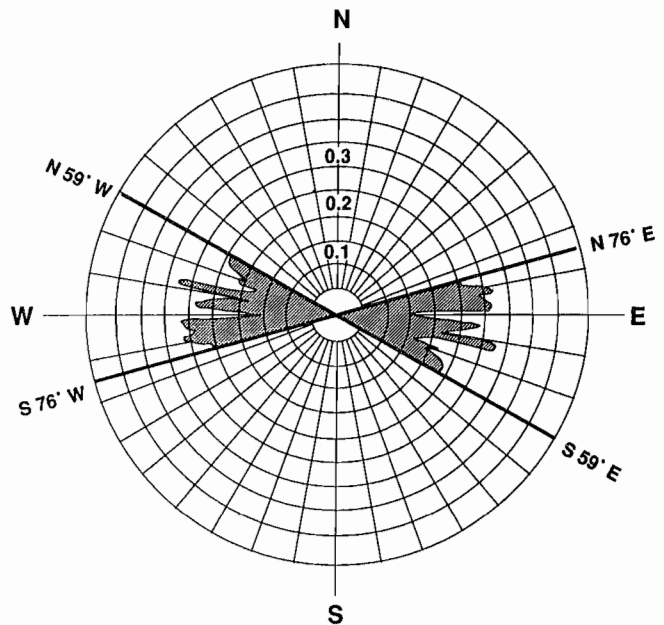


Figure 28.—Direction of ground water velocity with associated concentrations (in ppm) of plume as calculated by PLUME model.

the major controlling factor in determining the concentration of a lixiviant plume. As dispersivity was increased, peak concentration declined exponentially (fig. 30). Fracture spacing was found to have a large effect on dispersivity and, as a consequence, on peak concentration. As the spacing between fractures increased, concentration exponentially decreased (fig. 31); therefore, dispersivity increased. Fractures were assumed to be evenly spaced at 1-ft intervals for the base-case model. Dispersivity was conservatively assumed to be low (between 0.1 and 1 ft) at the site for the model because of the dense spacing. Low ground water velocities, under 20 ft/yr, gave high concentrations of the plume (fig. 32). At very high velocities, a lixiviant would disperse quickly to almost negligible concentrations within a few months. If the plume was traveling at a velocity of 20 ft/yr as opposed to 100 ft/yr, its concentration would decline from 150 ppm to 1.18 ppm after 1 year, compared with 0.24 ppm at 100 ft/yr. By the time the plume traveled the distance to the Big Five Tunnel, approximately 2,000 feet from the source, its concentration would be virtually undetectable.

To calculate the velocity of ground water flow in the base case, a gradient of 10^{-2} was used. This gave a velocity of 0.27 ft/d. The gradient between the site and the tunnel is approximately 10^{-1} . The water table is located below the slope, giving a gradient of less than 10^{-1} . Therefore, the gradient of 10^{-2} was assumed to be a reasonable estimate. The steeper gradient would have given a velocity of

2.7 ft/d. The trend in figure 32, shows that this higher velocity translates to lower concentrations.

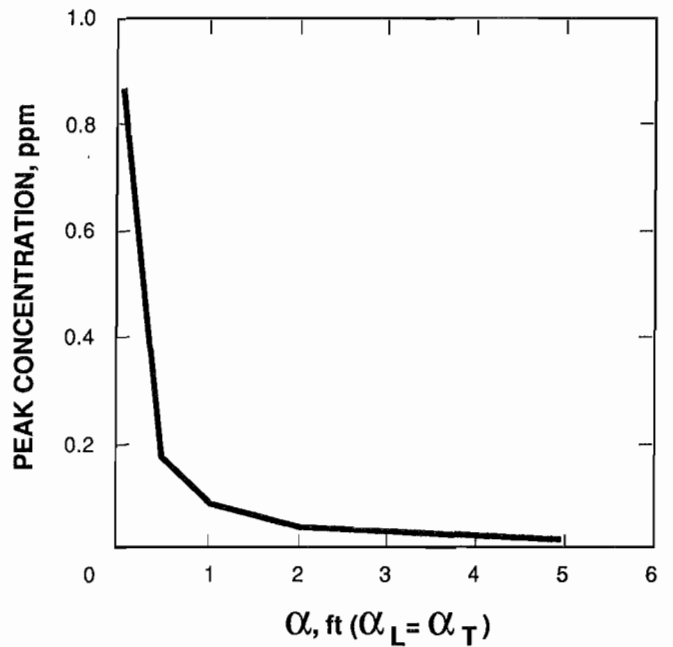


Figure 30.—Peak concentration versus dispersivity after 1 year.

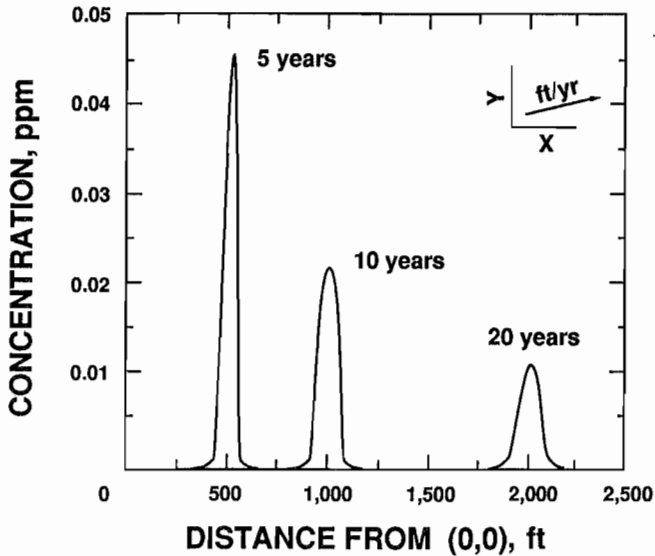


Figure 29.—Concentration versus distance with time as third variable.

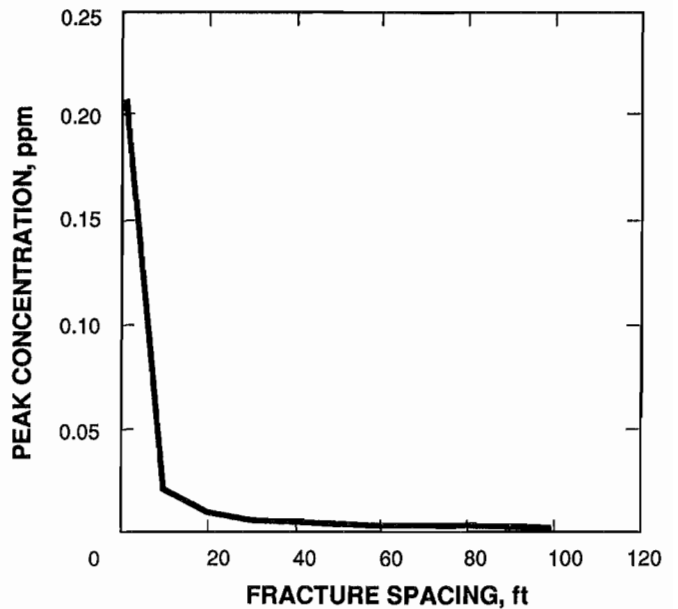


Figure 31.—Peak concentration versus fracture spacing after 1 year.

Peak concentration was sensitive to high porosities (fig. 33). A porosity of 100% would have given the highest peak concentrations. A porosity of 10% was used to run the base-case model, which was approximated from observations of fractures in the core. However, porosities of 4×10^{-1} to 1×10^{-4} were reported for the Edgar Mine (24). When these low porosities were used in the model, dispersivities were so high that only a trace of the lixiviant could be measured after a short time.

The model was run assuming that there was no adsorption or absorption onto or into the fracture walls by the lixiviant. Also, in the field, a lixiviant could reside in deadend fractures and never contribute to the plume. Therefore, the plume would actually be smaller and have lower concentrations of lixiviant than predicted by the model. In the field, ground water velocity and porosity would not be constant; therefore, dispersivities would vary. Another consideration is that the plume would not take a direct straight path of 2,000 ft to the tunnel: The direction of the path could vary.

Although the use of a lixiviant is not planned for this site, the following describes the flow pattern a lixiviant is likely to take away from the stope site. A majority of the flow in close proximity to the stope would likely flow in a westerly direction, as calculated by the PLUME model (fig. 28). This would be the predominant direction until the flow encountered a large fracture, vein, or other major discontinuity. The flow characteristics of the rock mass are controlled by geologic structure and by pressures induced by major discontinuities. This is based on the fact that flow in the area is controlled by structure and that most veins in the vicinity of the Edgar Mine strike northeast-southwest and dip to the northwest. In addition, many of the mined veins drain into the Big Five Tunnel (fig. 34), which was the purpose of the tunnel. After analyzing fracture patterns in the region and looking at the hydrologic history of the mining district, it was judged that the most likely path of fluid flow would be in the direction perpendicular to the strike of fractures, along fracture

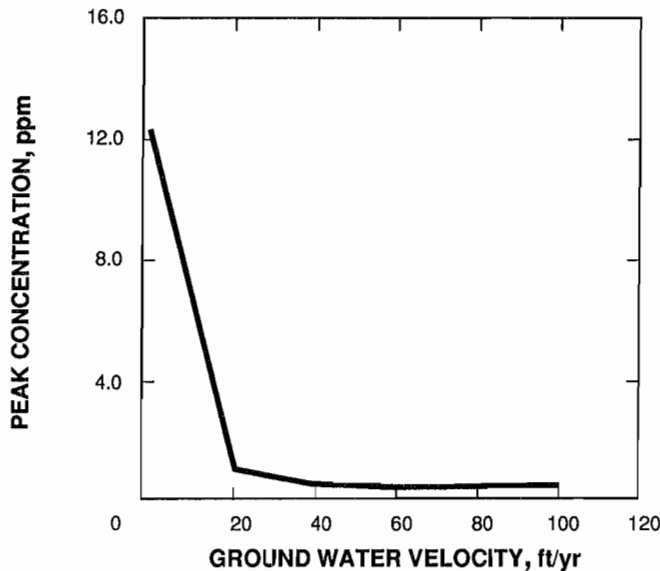


Figure 32.—Peak concentration versus ground water velocity after 1 year.

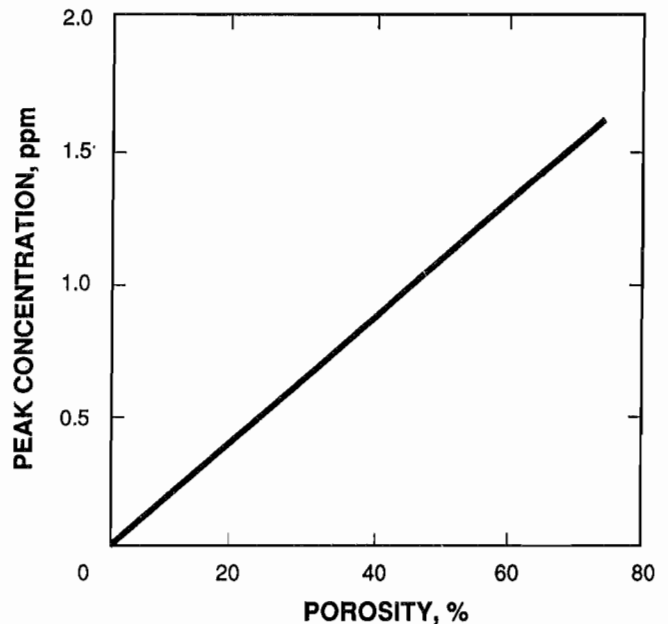


Figure 33.—Peak concentration versus porosity after 1 year.

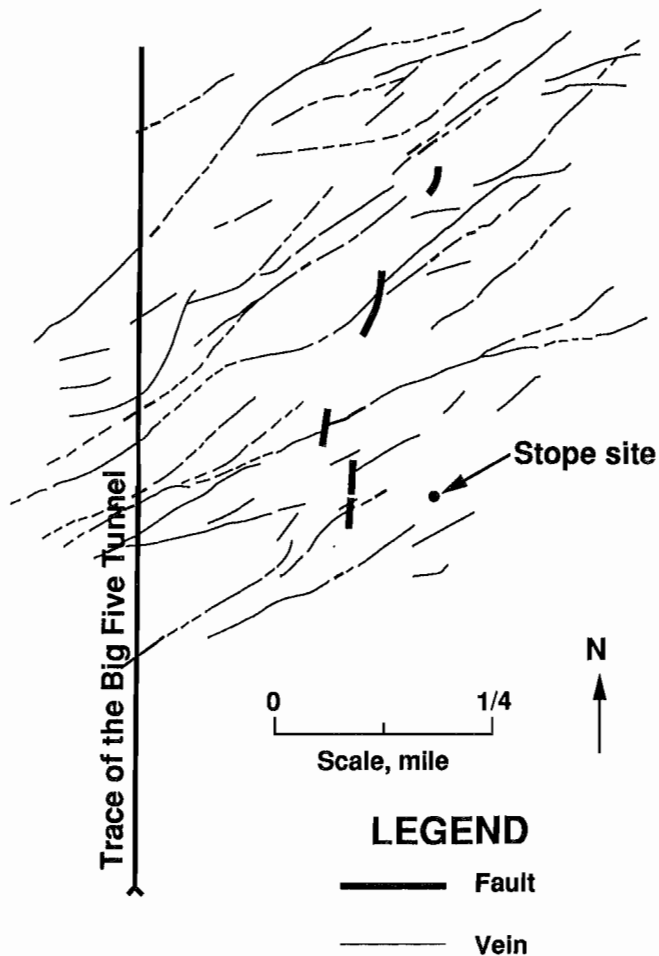


Figure 34.—Map of Idaho Springs area showing Big Five Tunnel, fault, and vein locations.

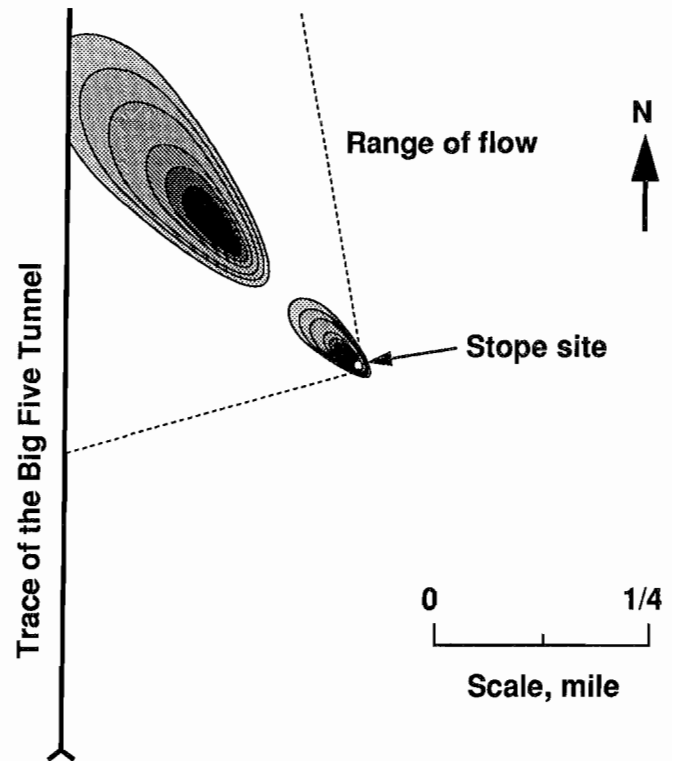


Figure 35.—Predicted flow direction of lixiviant plume (the dimensions of the plume are greatly exaggerated).

planes and veins, and toward the Big Five Tunnel, in a northwesterly direction. Figure 35 shows a likely area a lixiviant plume escaping from the stope site could cover, assuming flow is in the direction predicted by the model and along fracture planes.

CONCLUSIONS AND RECOMMENDATIONS

To characterize and model the fracture hydrology adjacent to an underground stope to be used for leaching ore, all available information on fracture characteristics in the Idaho Springs area and Edgar Mine were compiled and evaluated. These were crucial to predicting regional flow. For local flow evaluation, the geology of the stope area was mapped in detail, with special attention given to fracture characteristics. Fractures were also logged from 80 ft of core obtained from the stope area. This was collected and evaluated using statistical methods to determine if the sample was adequate to infer that the entire rock mass was similar to the sample for modeling purposes.

Structural features were found to be closely related to the regional hydrologic system. The fractures, on a local scale, and natural and manmade discontinuities, on a regional scale, were believed to be instrumental in directing flow of fluids within the rock mass.

To evaluate the fractures at the site, permeabilities of the fractures adjacent to and at the stope room were obtained using both air and water tests. Although the two media gave different results, a comparison of the two was conducted to find their applicability to future projects. As expected, the water permeability results were the most accurate.

Both the continuum and noncontinuum models were evaluated for application to the problem of an escaping lixiviant plume in a fractured rock mass. The de Josselin de Jong model, a continuum model, was thought to best support the geologic characteristics associated with the project. A computer model, PLUME, was used to evaluate flow within the rock mass. The PLUME model is based on the de Josselin de Jong fracture flow model.

A tracer test was conducted to evaluate particle transport in the rock mass adjacent to the stope site.

Although the test was questionable in describing lixiviant transport, it illustrated the control discontinuities have in intercepting flow.

The collected data and information were input into the PLUME model to find the likely paths a lixiviant may travel adjacent to the stope area and the concentrations of a lixiviant along a path. On a regional scale, however, this analytical computer model was not applicable. Flow on this scale is controlled by major veins and faults. Therefore, a discrete fracture model was conceptualized to evaluate the regional lixiviant flow.

It was concluded that an in situ stope leaching project would most likely be conducted in a mineralized region that had been extensively mined. In other words, the region would have many natural as well as manmade discontinuities. By nature, fluid in a rock mass will flow toward a major discontinuity located at the lowest elevation, such as a drainage or haulage tunnel. Even if the fluid reaches a discontinuity along its path of flow, some of the fluid may find its way to the ground water or surface water in the region eventually. The effects on the environment depend on the volume and concentration of the lixiviant reaching the resource. In the case of the hypothetical leaching project, it was predicted that the concentration of the lixiviant would range from near zero to 0.01 ppm after 20 years, traveling approximately 2,000 ft from the source. A concentration of 0.01 ppm was calculated assuming certain field conditions were not present, such as dead-end fractures, absorption, adsorption, and variable rock mass properties. These conditions would give smaller concentrations than those calculated. Additional tracer tests would give better estimates of these field conditions.

Geologic and hydrologic data coupled with modeling were essential in evaluating migration of the plume. The research conducted at the Edgar Mine site predicted that an escaping lixiviant plume would travel in a westerly direction. The plume would likely intercept a fault or mineralized vein. These features would probably direct the flow in a northwesterly direction toward the Big Five

Tunnel. Once in the tunnel, the effluent would drain into Clear Creek. Because of dispersion, the concentration of the lixiviant is expected to be relatively small by the time it reaches the tunnel. The more that is known about how a lixiviant plume can escape into the surrounding rock mass, the easier it is to control the process and prevent an accident.

For future investigations concerning data acquisition for modeling flow through fractures in a crystalline rock mass, it is recommended that several modifications be made in characterizing the rock mass. It has been suggested that cross-hole packer tests be run in addition to the single-hole packer tests. The cross-hole tests would determine which fractures are connected, and the hydraulic conductivities of specific fractures could be estimated.

A tracer test should be performed early in the hydrologic investigation. The earlier this test is performed, the better the chance of getting more accurate in situ dispersion measurements, because there would be fewer discontinuities and disturbances with which to contend. A tracer test could be used to determine fracture characteristics to which concentration is sensitive, such as porosity and ground water velocity.

Research on how the lixiviant behaves in the rock mass with respect to leaching is necessary. An escaping lixiviant may leach metals and minerals contained within the fractures and, therefore, widen fracture apertures. By leaching metals, the lixiviant could become rich in hazardous metals and/or these metals could precipitate within the fractures, eventually reducing the aperture of the fractures.

Sites where this method could be applied would most likely be unsaturated or partially saturated. Once leaching is commenced, the relationship between the degree of saturation and permeability will change, making this research very complex to model.

Since flow through fractures is a function of normal stress, shear stress, and fracture characteristics (17-18), it would be beneficial to measure the in situ stresses on fractures in a study area to better assess flow characteristics.

REFERENCES

1. Baecher, G. B., N. A. Lanney, and H. H. Einstein. Statistical Description of Rock Properties and Sampling. Paper in Proceedings, 18th U.S. Symposium on Rock Mechanics. CO Sch. Mines Press, 1977, pp. 5C1-8.
2. Barton, C. M. Geotechnical Analysis of Rock Structure and Fabric in C.S.A. Mine, Cobar, New South Wales. Appl. Geomech. Tech. Pap. 24, Common. Sci. and Ind. Res. Organ., Australia, 1977.
3. Bear, J. Dynamics of Fluids in Porous Media. Am. Elsevier, New York, 1972, 754 pp.
4. Bridges, M. C. Presentation of Fracture Data for Rock Mechanics. Paper in 2nd Australia-New Zealand Conference on Geomechanics (Brisbane). 1975, pp. 144-148.
5. Call, R. B., J. Savely, and D. E. Nicholas. Estimation of Joint Set Characteristics From Surface Mapping Data. Paper in Proceedings, 17th U.S. Symposium on Rock Mechanics. UT Eng. Exper. Stn., 1976, pp. 2B2-1-2B2-9.
6. Cameron, R. Investigation and Geophysical Testing on Excavation of a Tunnel Test Site Under BRRDEC Tunnel Detection Program. Unpubl. rep. for U.S. Army, Belvoir Res., Dev., and Eng. Cent. by Dep. Min. Eng., CO Sch. Mines, Golden, CO, 1987, 32 pp; available upon request from N. Miller, BuMines, Denver, CO.
7. Camp Dresser and McKee, Inc. Letter Report, Supplemental Data on Tunnels, Clear Creek/Central City Site, Project 2687 for

- Gormley Consultants Inc., CO. Oct. 1988, 13 pp; available from Superfund Records Cent., EPA, Region VIII, Denver, CO.
8. Camp Dresser and McKee, Inc. Final Draft, Remedial Investigation Report, Addendum No. 2, Clear Creek/Central City Site (U.S. EPA contract 68-01-6939). Aug. 1988, 133 pp; available from Superfund Records Cent., EPA, Region VIII, Denver, CO.
 9. Chandrasekhar, S. Stochastic Problems in Physics and Astronomy. *Rev. Mod. Phys.*, v. 15, 1943, pp. 1-87.
 10. Cruden, D. M. Describing the Size of Discontinuities. *Int. J. Rock Mech. and Min. Sci.*, v. 14, 1977, pp. 133-137.
 11. Darcy, H. *Les Fontains Publiques de la Ville de Dijon* (The Public Fountains of the City of Dijon). Victor Dalmont, Paris, 1856, 647 pp.
 12. De Josselin de Jong, G. Dispersion of a Point Injection in an Anisotropic Medium. Unpubl. rep., NM Inst. Min. and Technol., Socorro, 1972, 68 pp; available upon request from N. Miller, BuMines, Denver, CO.
 13. De Josselin de Jong, G., and S. C. Way. Dispersion in Fissured Rock. Unpubl. rep., NM Inst. Min. and Technol., Socorro, 1972, 30 pp; available upon request from N. Miller, BuMines, Denver, CO.
 14. Einstein, H. H. Risk Analysis for Rock Slopes in Open Pit Mines—Part I and IV (contract J02575015). MIT, 1979.
 15. Florquist, B. A. Techniques for Locating Water Wells in Fractured Crystalline Rocks. *Ground Water*, v. 11, No. 3, 1973, pp. 26-28.
 16. Freeze, A. R., and J. A. Cherry. *Groundwater*. Prentice-Hall, 1979, 604 pp.
 17. Gale, J. E. Assessing the Permeability Characteristics of Fractured Rock. *Geol. Soc. Am., Spec. Pap.*, 1982, 19 pp.
 18. Gertsch, L. S. Coupled Deformation and Fluid Flow Behavior of a Natural Fracture in the CSM In Situ Test Block. Ph.D. Dissertation, CO Sch. Mines, Golden, CO, 1989, 1985 pp.
 19. Harrison, J. E., and R. H. Moench. Joints in Precambrian Rocks Central City-Idaho Springs Area, Colorado. U.S. Geol. Surv. Prof. Pap. 374-B, 1961, 14 pp.
 20. Hubbert, M. K. Darcy's Law and the Field Equations of the Flow of Underground Fluids. Ch. in *Petroleum Transactions*. AIME, Tech. Pap. 4352, 1956, pp. 222-239.
 21. Hull, L. C. Physical Model Studies of Dispersion in Fracture Systems. U.S. Dept. Energy, Idaho Operations Office, E. G. & G. Idaho, Inc., Apr. 1985, 9 pp.
 22. Hutchinson, R. M. Geological and Structural Setting of the CSM/OCRD Test Site: CSM Experimental Mine, Idaho Springs, Colorado. Tech. Rep., CO Sch. Mines, Golden, CO, Sept. 1983, 47 pp.
 23. In-situ Inc., Computer Technology Division (Laramie, WY). Software and "PLUME" User's Guide. V2.1, Dec. 1986, 44 pp.
 24. INTERA Environmental Consultants, Inc. (Houston, TX). Porosity, Permeability, and Their Relationship in Granite, Basalt, and Tuff. Tech. Rep. ONWI-458, Apr. 1983, 63 pp.
 25. Karadi, A. M., R. J. Krizek, and E. Castillo. Hydrodynamic Dispersion in a Single Rock Joint. *J. Appl. Phys.*, v. 43, No. 12, 1972, pp. 5013-5021.
 26. Katz, D. L., D. Cornell, R. Kobayashi, F. H. Poettmann, J. A. Vary, J. R. Elenbaas, and C. F. Weinaug. *Handbook of Natural Gas Engineering*. McGraw-Hill, New York, 1959, pp. 43-46.
 27. Kulatilake, P. H. S. W. Stochastic Joint Geometry Modelling: State of the Art. Paper in Proceedings of the 29th U.S. Symposium on Rock Mechanics (Minneapolis, MN). Balkema, 1988, pp. 215-229.
 28. Kunkel, J. R., S. C. Way, and C. R. McKee. Calculation of Dispersion in Saturated Fractured Geologic Media. Unpubl. rep., 1988, 17 pp.; available upon request from N. Miller, BuMines, Denver, CO.
 29. _____. Comparative Evaluation of Selected Continuum and Discrete-Fracture Models. U.S. Nucl. Reg. Comm., NUREG/CR-5240, 1988, 61 pp.
 30. Moench, R. H., and A. A. Drake. Economic Geology of the Idaho Springs District, Clear Creek and Gilpin Counties, Colorado. U.S. Geol. Surv. Bull. 1208, 1966, 91 pp.
 31. Montazer, P. Permeability of Unsaturated, Fractured Metamorphic Rocks Near an Underground Opening. Ph.D. Dissertation, CO Sch. Mines, Golden, CO, Nov. 1982, 447 pp.
 32. Paschis, J. A., J. R. Kunkel, and R. A. Koenig. Well Field Installation and Investigations, Creston Study Area, Eastern Washington. U.S. Nucl. Reg. Comm. NUREG/CR-5251, 1988, 109 pp.
 33. Priest, S. D., and J. Hudson. Discontinuity Spacings in Rock. *Int. J. Rock Mech. and Min. Sci.*, v. 18, 1976, pp. 135-148.
 34. Ramey, H. J., Jr., R. G. Agarwal, and I. Martin. Analysis of "Slug Test" or DST Flow Period Data. *J. Can. Pet. Technol.*, July-Sept. 1975, pp. 37-47.
 35. Robertson, A. The Interpretation of Geological Factors for Use in Slope Stability. Pres. at Symposium on the Theoretical Background to the Planning of Open Pit Mines, With Special Reference to Slope Stability. S. Afr. Inst. Min. and Metall., Johannesburg, 1970; available upon request from N. Miller, BuMines, Denver, CO.
 36. Schwartz, F. W., and L. Smith. A Continuum Approach for Modeling Mass Transport in Fractured Media. *Water Resour. Res.*, v. 24, No. 8, Aug. 1988, pp. 1360-1372.
 37. Sen, Z., and A. Kazi. Discontinuity Spacing and RQD Estimates From Finite Length Scanlines. *Int. J. Rock Mech. and Min. Sci.*, 1984, v. 21, pp. 203-212.
 38. Smith, L., and F. W. Schwartz. An Analysis of the Influence of Fracture Geometry on Mass Transport in Fractured Media. *Water Resour. Res.*, v. 20, No. 9, Sept. 1984, pp. 1241-1252.
 39. Snow, D. T. Anisotropic Permeability of Fractured Media. *Water Resour. Res.*, v. 5, No. 6, Dec. 1969, pp. 1273-1289.
 40. _____. Fracture Deformation and Changes of Permeability and Storage Upon Changes of Fluid Pressure. *Q. CO Sch. Mines*, v. 63, No. 1, 1968, pp. 201-244.
 41. _____. Rock Fracture Spacings, Openings, and Porosities. *J. Soil Mech. and Foundations Div. (Proc. Am. Soc. Civ. Eng.)*, Jan. 1968, pp. 99-117.
 42. Steffen, O. Recent Developments in the Interpretation of Data From Joint Surveys in Rock Masses. Proceedings of the 6th Conference for Africa on Soil Mechanics and Foundations. V. II, 1975, pp. 17-26.
 43. Streeter, V. L. *Fluid Mechanics*. McGraw-Hill, 1971, pp. 233-235.
 44. Wallis, P. F., and M. S. King. Discontinuity Spacings in Crystalline Rock. *Int. J. Rock Mech. and Min. Sci.*, v. 17, 1980, pp. 63-66.
 45. Way, S. C., and C. R. McKee. Restoration of In Situ Coal Gasification Sites From Naturally Occurring Groundwater Flow and Dispersion. Univ. WY, Laramie, WY. In-Situ Rep. No. 5(2), 1981, pp. 77-101.
 46. Witherspoon, P. A., J. S. Y. Wang, K. Isai, and J. E. Gale. Validity of Cubic Law for Fluid Flow in a Deformable Rock Fracture. *Water Resour. Res.*, v. 16, No. 6, Dec. 1980, pp. 1016-1024.